Long-term trends in pH in Japanese coastal seawater

Miho Ishizu[1], Yasumasa Miyazawa[1], Tomohiko Tsunoda[2], Tsuneo Ono[3]

[1]E-mail: mishizu@jamstec.go.jp

[1]E-mail: miyazawa@jamstec.go.jp

Japan Agency for Marine-Earth Science and Technology, Environmental Variability Prediction and Application Research Group, Yokohama Institute for Earth Sciences, 3173-25 Showa-machi, Kanagawa-ku, Yokohama 236-0001, Japan

Tel: +81-45-778-5875

Fax: +81-45-778-5497

[2]E-mail: t-tsunoda@spf.or.jp

The Ocean Policy Research Institute of the Sasakawa Peace Foundation, 1-15-16, Toranomon Minato-ku, Tokyo 105-8524, Japan

[3]E-mail: tono @affrc.go.jp

Japan Fisheries Research Education Agency, 15F Queen's Tower B, 2-3-3 Minato Mirai, Nishi-ku, Yokohama, Kanagawa 220-6115, Japan

Abstract

In recent decades, acidification of the open ocean has shown consistent increases. However, analysis of long-term data in coastal seawater shows that the pH is highly variable because of coastal

processes and anthropogenic carbon inputs. It is therefore important to understand how anthropogenic carbon inputs and other natural or anthropogenic factors influence the temporal trends in pH in coastal seawater. Using water quality data collected at 289 monitoring sites as part of the Water Pollution Control Program, we evaluated the long-term trends of the pH_{insitu} in Japanese coastal seawater at ambient temperature from 1978 to 2009. We found that the annual maximum pH_{insitu}, which generally represents the pH of surface waters in winter, had decreased at 75% of the sites, but had increased at the remaining sites. The temporal trend in the annual minimum pH_{insitu}, which generally represents the pH of subsurface water in summer, also showed a similar distribution, although it was relatively difficult to interpret the trends of annual minimum pH_{insitu} because the sampling depths differed between the stations. The annual maximum pH_{insitu} decreased at an average rate of −0.0024 yr^{-1}, with relatively large deviations (0.0042 yr^{-1}) from the average value. Detailed analysis suggested that the decrease in pH was caused partly by warming of winter surface waters in Japanese coastal seawater. The pH normalized to 25°C, however, showed decreasing trends, suggesting that dissolved inorganic carbon from anthropogenic sources was increasing in Japanese coastal seawater.

Keywords: pH, CO_2, Global warming, Ocean acidification, Coastal acidification/basification, Data analysis

1. Introduction

The effect of ocean acidification on several marine organisms, including calcifiers, is widely acknowledged and is the topic of various marine research projects worldwide. Chemical variables related to carbonate cycles are monitored in several ongoing ocean projects to determine whether the rate of ocean acidification can be identified from changes in pH and other variables in the open ocean (Gonzalez-Davila et al. 2007; Dore et al. 2009; Bates 2007; Bates et al. 2014; Midorikawa et al. 2010; Olafsson et al. 2009; Wakita et al. 2017). Analysis of pH data measured in situ at the European Station in the Canary Islands (ESTOC) in the North Atlantic from 1995 to 2003 and normalized to 25 °C showed that the pH_{25} decreased at a rate of 0.0017±0.0005 yr^{-1} (Gonzalez-Davila et al. 2007). Similarly, analysis of the Hawaii Ocean Time series (HOT) (Dore et al. 2009) and the Bermuda Atlantic Time Series (BATS) (Bates 2007) showed that the pH at ambient (in situ) sea surface temperature (pH_{insitu}) decreased by 0.0019±0.0002 and 0.0017±0.0001 yr^{-1} from 1988 to 2007 and from 1983 to 2005, respectively. Analysis of data collected along the hydrographic observation line at 137°E in the western North Pacific by the Japanese Meteorological Agency (JMA) showed that the pH_{25} decreased by 0.0013±0.0005 yr^{-1} in summer and 0.0018±0.0002 yr^{-1} in winter from 1983 to 2007 (Midorikawa et al. 2010). The winter pH_{insitu} in surface water in the Nordic Seas decreased at a rate of 0.0024±0.0002 yr^{-1} from 1985 to 2008 (Olafsson et al. 2009). This rate was somewhat more rapid than the average annual rates calculated for the other subtropical time series in the Atlantic Ocean, BATS, and ESTOC, and was attributed to the higher air–sea CO_2 flux and lower buffering capacity (higher Revell factor) (Olafsson et al. 2009). Wakita et al. (2017) estimated that the annual and winter pH_{insitu} at station K2

62 in the subarctic western North Pacific decreased at rates of 0.0025 and 0.0008 yr^{-1}, respectively, from
63 1999 to 2015. The lower rate in winter was explained by increases in dissolved inorganic carbon (DIC)
64 and total alkalinity (Alk) that resulted from climate-related variations in ocean currents.

65 These long-term time series from various sites in the open ocean indicate consistent changes in
66 surface ocean carbon chemistry, which mainly reflect the uptake of anthropogenic CO_2, with
67 consequences for ocean acidity. Coastal seawater, however, differ from the open ocean as they are
68 subjected to multiple influences, such as hydrological processes, land use in watersheds, nutrient inputs
69 (Duarte et al. 2013), changes in the structure of ecosystems caused by eutrophication (Borges and
70 Gypens 2010; Cai et al. 2011), marine pollution (Zeng et al. 2015), and variations in salinity (Sunda
71 and Cai 2012).

72 Duarte et al. (2013) hypothesized that anthropogenic pressures would cause the pH_{insitu} of coastal
73 seawater to decrease (acidification) or increase (basification), depending on the balance between the
74 atmospheric CO_2 inputs and watershed exports of alkaline compounds, organic matter, and nutrients.
75 For example, in Chesapeake Bay, the pH_{insitu} has shown temporal variations over the last 60 years,
76 presumably because of the combined influence of increases and decreases in pH_{insitu} in the mesohaline
77 and polyhaline regions of the main part of the bay, respectively (Waldbusser et al., 2011; Duarte et al.,
78 2013).

79 These processes that occur only in coastal regions might cause increases or decreases in the rate of
80 acidification, meaning that the outcomes for coastal ecosystems in different regions will vary. At

present we have limited information about long-term changes in pH in coastal seawater, mainly because of the difficulty involved in collecting continuous long-term data from coastal seawater around an entire country at a spatial resolution that sufficiently covers the high regional variability in coastal pH.

The Water Pollution Control Law (WPCL) was established in 1970 to deal with the serious pollution of the Japanese aquatic environment in the 1950s and 1960s. Several environmental variables, including pH_{insitu}, have been continuously measured in coastal waters since 1978, using consistent methods enacted in the monitoring program under the leadership of the government, to help protect coastal water and groundwater from pollution and retain the integrity of water environments. The errors in pH measurements collected in this program were assessed as outlined in the JIS Z8802 (JIS; Japanese Industrial Standard) standard protocol (2011) that corresponds to the ISO 10523 (ISO; International Organization for Standardization) standard protocol. Compared with the specialized oceanographic protocols described in the United States Department of Energy (DOE) Handbook (1994), it is not difficult to achieve the JIS protocol. The JIS and DOE standard protocols allow measurement errors of less than ±0.07 and ±0.003, respectively, for the glass electrode method, and the DOE protocol demands a precision of ±0.001 for the spectrophotometric method. Measurements are generally made with the higher-quality spectrophotometric method during major oceanographic studies (e.g. Midorikawa et al. 2010).

Regardless of any shortcomings, the WPCL coastal monitoring program in Japan includes more

than 2000 monitoring sites that cover most parts of the coastline (Fig. 1), so the dataset provides the opportunity to estimate the overall trend in pH in Japanese coastal areas and the regional variability in the trends from data of known precision. Suitable analytical methods could make up for these shortcomings of the WPCL dataset. In this study, we focused on the general characteristics of the overall pH trends at the all monitoring sites rather than examining the trend in pH at each site in detail, after carefully considering the accuracy of the dataset.

In the present study, we examined the pH_{insitu} trends in surface coastal seawater from data measured as part of WPCL monitoring programs. We then examined the trends at specific locations. The remainder of this manuscript is organized as follows: the data and methods are described in Section 2, and trends in pH_{insitu} are presented in Section 3, the results are discussed in Section 4, and the concluding remarks are provided in Section 5.

2. Materials and Methods

2.1 Water Pollution Control Law (WPCL) monitoring data

Data for several environmental variables, including pH_{insitu}, and the associated metadata, are available on the website of the National Institute for Environmental Studies (NIES) (www.nies.go.jp/igreen; http://www.nies.go.jp/igreen/md_down.html). We downloaded pH_{insitu} data from 1978 to 2009 for the trend analysis. We also downloaded temperature (T) and total nitrogen (TN) data that were measured at the same sites as the pH_{insitu} data for the same time period (data for T and

119 TN were available from 1981 to 2006, and from 1995 to 2009, respectively), to check the quality of
120 the pH_{insitu} data (Section 2.2).

121 The data were collected by the Regional Development Bureau of the Ministry of Land,
122 Infrastructure, Transport and Tourism, and the Ministry of the Environment under the WPCL
123 monitoring program. Monitoring protocols (sampling frequencies, locations, and methods) are outlined
124 in the program guidelines (NIES 2018; Ministry of Environment (MOE) 2018) written in Japanese,
125 and we have provided a summary of these protocols in this manuscript.

126 Monitoring is carried out at 1481 sites along the Japanese coasts, as shown in Figure 1a. While
127 most sites are in coastal sea areas, up to 10% are in estuaries. At each monitoring site, basic surveys
128 were carried out between 4 and 40 times a year, depending on the site. Information on the sampling
129 frequency at the monitoring sites is presented in Table 1. During basic surveys, water samples were
130 collected from 0.5 and 2.0 m below the surface at all sites; at sites where the bottom depths were
131 greater than 10 m. Water samples were collected four times a day to cover diurnal variation. At sites
132 where the variation in the daily pH was large, samples were also collected over a period of one day at
133 2-hourly intervals (ca. 13 times a day) at least twice a year to check the adequacy of the basic water
134 sampling protocol.

135 The pH for each water sample was measured in accordance with the Japanese Industrial Standard
136 protocol JIS Z 8802 (2011), which is equivalent to ISO10523
137 (https://www.iso.org/standard/51994.html). The pH was measured by glass electrode calibrated by

NBS standard buffers. The electrode and pH-meter had to produce measurements that were repeatable to ±0.05. The pH was measured immediately after the water samples were collected, at the ambient water temperature. The repeatability permitted in each measurement was ±0.07. The pH data were collected by the environmental bureau of each prefectural government, which reported only annual minimum and maximum pH values at each station to the MOE, because the original purpose of the WPCL program was to monitor whether the annual variations in water properties (in this case pH) were within ranges set by the national environmental quality standard. The published WPCL pH dataset therefore contains only these annual minimum and maximum pH data in each year, reported on the NBS pH scale (pH_{insitu}) and rounded to one decimal place. Water temperature data are also available for each sampling event (http://www.nies.go.jp/igreen/md_down.html). Previous studies have reported negative correlations between seasonal variations in pH and water temperature, mainly because of changes in the dissociation constants of carbonate and bicarbonates (Millero 2013); the pH values were lowest in summer and highest in winter, in both stations in low- and mid-latitudes of the north hemisphere in the open ocean (e.g. Bates et al. 2014) and coastal seawater (e.g., Frankignoulle and Bouquegneau 1990; Byrne et al. 2013; Hagens et al. 2015; Challener at al. 2016). We therefore assumed that the minimum and maximum pH data coincided with the highest and lowest temperatures, respectively (Fig. 2), and we used these data to calculate the pH_{25} in Section 4.2.

The monitoring operations were carried out by licensed operators as outlined in the annual plan of the Regional Development Bureau of each prefecture. These specific licensed operators were retained

157 for the duration of the measurement period, which means that the same laboratories were always in
158 charge of collecting the data. This approach helps to prevent systematic errors that might arise both
159 between measurement facilities and over time, and ensures the datasets are accurate.
160
161 2.2 Quality control procedures and assessing the consistency of the WPCL monitoring data
162 We selected all the data for fixed sites in coastal seawater that had continuous time series from
163 1978 to 2009. There were 2463 regular and non-regular monitoring sites in 1978 and 2127 sites in
164 2009. While there were very few sites in some prefectures in Hokkaido and Tohoku, the monitoring
165 sites covered almost all the coastline in Japan (Fig. 1).
166 As explained in more detail later in this section, we applied a three-step quality control procedure.
167 We excluded 1) discontinuous time sequences, 2) time sequences that had extreme outliers in each year,
168 and 3) time sequences that included significant random errors, and which were only weakly correlated
169 with time sequences at adjacent sites.
170 When we excluded the sites that had discontinuous pH_{insitu} time sequences from 1978 to 2009, 1481
171 sites remained (Fig. 1). We then excluded time sequences with outliers, defined as sites with data points
172 that were more than three standard deviations from the average of minimum and maximum pH_{insitu}
173 values for each year. After this step, 1127 sites remained (not shown). We calculated the trends in the
174 unbroken continuous time sequences of the minimum and maximum pH_{insitu} data at each site with
175 linear regression (Fig. 3), and the slopes of the linear regression were taken as the minimum and

maximum pH_{insitu} trends (e.g. Fig. 3). The linear regression trends might have been influenced by random errors or variations at different temporal scales in the data for each site. To eliminate the influence of these errors and variations as far as possible, we removed the data that had significant random errors, defined as the time sequences for which the standard deviations of pH_{insitu} exceeded the average standard deviation of the pH_{insitu} time sequences at the 1127 sites. After this step, 302 sites remained (see Fig. 1b for site locations).

For the 302 sites, we evaluated whether the water temperature (Fig. 4a−b) and pH_{insitu} (Fig. 4c−d) were correlated at adjacent monitoring sites in the same prefecture (Fig. 4). At most of the stations, the correlations between the temperatures at the site pairs were relatively strong, which indicates that the temperature followed similar patterns over time at adjacent sites (Fig. 4a−b). The correlations tended to be strong when the sites were close together, but gradually weakened with increasing distance between sites. The pH_{insitu} correlations followed a similar pattern (Fig. 4), which indicates that the pH_{insitu} and temperature data at adjacent monitoring sites varied in the same way. In other words, the relative ratios of the measurement errors in pH_{insitu} and the natural spatio-temporal variations at these monitoring sites were similar to those for temperature. The absolute values of the correlation coefficients for the pH_{insitu} were slightly lower than those for temperature for each corresponding pair of sites (Figs. 4 and 5), and might reflect the fact that pH_{insitu}, but not the water temperature, is subjected to strong forcing by coastal biological processes and other severe physical processes in summer, which causes the pH_{insitu} to vary on the short-term. The correlations between the minimum pH_{insitu} data (Fig.

195 4c) were weaker than those for the maximum pH_{insitu} data (Fig. 4d) because the degree of biological
196 forcing varied by season and was stronger in summer when the pH_{insitu} was at a minimum and weaker
197 in the winter when the pH_{insitu} was at a maximum. Despite the influence of biological processes on the
198 pH_{insitu}, the correlation coefficients remained high and were significant ($\boldsymbol{r}$=0.367, p<0.05) at most of
199 the monitoring sites, especially at sites that were less than 5 km apart within the same prefecture, where
200 the pH_{insitu} followed similar patterns. In the final step of the quality check procedure (step 3), we
201 removed all the time sequences with weak and insignificant correlations for temperature and pH_{insitu}
202 (Fig. 5), because we considered that the monitoring sites having both significant correlations for water
203 temperature and pH_{insitu} were reliable. After this final step, 289 sites remained. As shown in Table 2,
204 the correlations between temperature and pH_{insitu} at sites within 15 km of each other strengthened after
205 steps 2 and 3, which suggests that the reliability of the dataset improved at each step of the quality
206 control.

207 The monitoring in each prefecture is carried out by different licensed operators, decided by the
208 Regional Development Bureau in each prefecture. Inter-calibration measurements have not been
209 conducted between different licensed operators. Even though all the operators follow the same JIS
210 protocol, manual monitoring can introduce systematic errors into the data. Some adjacent monitoring
211 sites are close to each other but are managed by different operators, such as sites close to the boundaries
212 between Osaka and Hyogo (Fig. 6a), Hyogo and Okayama (Fig. 6b), Kagawa and Okayama (not
213 shown), and Kagawa and Ehime (not shown). The pH_{insitu} time sequences for these site pairs were

generally similar, even though there were some deviations when compared with the time sequences for adjacent sites within the same prefecture, monitored by the same operator (lines of the same color in Fig. 6). The standard deviations of the pH_{insitu} trends between these site pairs close to the boundaries of Osaka and Hyogo, Hyogo and Okayama, Kagawa and Okayama, and Kagawa and Ehime were 0.0014, 0.0012, 0.0026, and 0.0017 yr^{-1}, respectively, and were smaller than the acceptable measurement errors of the JIS standard protocols. We can therefore assume that the measurements from the different operators in different prefectures were consistent.

3. Results

3.1 Variations in pH_{insitu} highlighted by regression analysis

The histograms of the calculated pH_{insitu} trends (yr^{-1}), for the minimum and maximum pH_{insitu} after each quality control step, are shown in Fig. 7. The histogram in Fig. 7a–b shows the data for the 1481 sites (discontinuous sites excluded). The data for the 1127 sites from step 2 (i.e., data without outliers) are shown in Fig. 7c–d, and the data for the 289 sites from step 3 are shown in Fig. 7e–f (Section 2.2). The number of sites decreased at each step of the quality control, but the shapes of the histograms were generally similar for both the minimum and maximum pH trends. The total trends showed overall normal distributions with a negative shift at all levels of quality control.

We detected both positive (basification) and negative (acidification) trends, which contrasts with the findings of other researchers who reported only negative trends (ocean acidification) in the open

233 ocean (Bates et al. 2014; Midorikawa et al. 2010; Olafsson et al. 2009; Wakita et al. 2017). The average
234 (±standard deviation) trends for the minimum and maximum pH_{insitu} data were −0.0002±0.0061 and
235 −0.0023±0.0043 yr^{-1} for the 1481 sites (Fig. 7a−b), and −0.0005±0.0042 and −0.0023±0.0036 yr^{-1} for
236 the 1127 sites (Fig. 7c−d), respectively. The average trends for the minimum and maximum pH_{insitu}
237 data for the 289 sites that remained after step 3 were −0.0014±0.0033 and −0.0024±0.0042 yr^{-1},
238 respectively (Fig. 7e−f).

239 The negative trends were relatively weak for the minimum pH_{insitu} data and relatively strong for
240 the maximum pH_{insitu} data, but there was an overall tendency towards acidification. At the 289 sites,
241 there were 204 negative and 86 positive trends for the minimum pH_{insitu} data and 217 negative and 72
242 positive trends for the maximum pH_{insitu} data. This shows that, for the minimum pH_{insitu} data, there
243 were acidification and basification trends at 70% and 30% of the monitoring sites, respectively, and at
244 75% and 25% for the maximum pH_{insitu} data, respectively.

245

246 3.2 Local patterns in acidification and basification

247 We examined the pH_{insitu} trends for the 289 sites for local patterns in acidification and basification
248 (Section 2.2) and found that the trends seemed to be randomly distributed. For example, the values
249 were different at sites that were less than 50 km apart (Fig. 8). There are many monitoring sites in the
250 Seto Inland Sea and in Western Kyushu. The trends for the minimum and maximum pH_{insitu} showed
251 both acidification and basification in the Seto Inland Sea (Fig. 8a−b, 8c−d). In the western part of

252 Kyushu, acidification dominated (Fig. 8a−b, 8c−d) with only basification in pH_{insitu} at a few sites for
253 both the minimum and maximum pH_{insitu} data (Fig. 8b, d). Figure 8a (b) and Figure 8c (d) are similar,
254 which suggests that, at most of the sites where we detected acidification and basification, the trend
255 directions were consistent for the minimum and maximum pH_{insitu} (Fig. 8a−b, 8c−d).

256 By examining the average minimum and maximum pH_{insitu} trends in each prefecture (Fig. 9a−b, d−e,
257 g−h, j−k), we found that, while the average values were slightly different, the trends in the averaged
258 values and the patterns in acidification and basification for both the minimum and maximum pH_{insitu}
259 were the same from north to south and from west to east. We also found acidification trends in most of
260 the prefectures with at least 17 sampling sites, namely Miyagi, Wakayama, Hyogo, Okayama,
261 Yamaguchi, Tokushima, Kagawa, Ehime, and Nagasaki (Figs. 1a and 9c, f, i, l). The average estimates
262 for the maximum pH_{insitu} were larger than those for the minimum pH_{insitu} in these prefectures.

263 We found more acidification trends for the minimum pH_{insitu} in the southwestern prefectures of
264 Yamaguchi, Kagawa, Ehime, Hyogo, and Nagasaki than in the northeastern prefecture of Miyagi (Fig.
265 9a, d, g, i) (see Fig. 1 for locations). The maximum and minimum pH_{insitu} trends indicated basification
266 in Wakayama and Okayama prefectures (Fig. 9c). The trends in Osaka, Hyogo, Okayama, Hiroshima,
267 Yamaguchi, Kagawa, and Ehime prefectures (Fig. 1a) were different, even though they were all located
268 in the same part of the Seto Inland Sea (Fig. 9d−e). The trends in Hiroshima and Okayama, within the
269 Seto Inland Sea, were weaker than those in Hyogo, Yamaguchi, Kagawa, and Ehime, which were
270 outside the sea (Fig. 9d−e). The pH_{insitu} trend values indicated relatively strong acidification at a rate

271 of −0.0025 yr^{-1} in Niigata in the Japan Sea (Fig. 9j−l) but there were fewer than the threshold of 17
272 monitoring sites in the prefectures.
273
274 # 4. Discussion
275 ## 4.1 Statistical evaluation of our estimated overall trends
276 The JIS Z8802 (2011) allows a measurement error of ±0.07 and this treatment further enhanced the
277 uncertainty of the published data to ±0.1. The uncertainty of the slope of the linear regression line (σ_β)
278 is estimated with the following equation (e.g., Luenberger 1969):
279 $$\sigma_\beta = \{\sigma^2_y / \Sigma(x_i-[x])^2\}^{1/2} \quad (1)$$
280 where σ^2_y is the theoretical variance in a pH value caused by the measurement error (in this case, 0.1^2
281 = 0.01); and x_i and [x] represent the year and the year averaged for all data at a station, respectively.
282 In the WPCL dataset, there are generally 32 data points for each station (for every year from 1978 to
283 2009), spaced at consistent intervals. In this case, $\Sigma(x_i - [x])^2$ becomes 2728 and σ_β becomes 0.0020
284 yr^{-1}, which is the threshold of significance for the pH trend. This means that our estimated trends
285 included standard deviations that were less than 0.0020 yr^{-1}, and, if there were no trends, a histogram
286 of the pH trends should be normally distributed with an average and standard deviation (σ_β) of 0.0000
287 and 0.0020 yr^{-1}, respectively (Fig. 7). The average trend in the maximum pH_{insitu}, however, shifted
288 from zero in a negative direction at a rate of more than 0.0020 yr^{-1} for all three scenarios (Fig. 7b, d,
289 f). This result implies that, averaged over the whole country, the Japanese coast was acidified in winter

290 to a degree that could be detected from the historical WPCL pH data, even with an uncertainty of ±0.1.
291 The observed standard deviation for the maximum pH_{insitu} was also larger than the expected value of
292 0.0020 yr^{-1} because of local variations in the pH trends. The average shift in the minimum pH_{insitu} data
293 was smaller than 0.0020 yr^{-1}, but all three scenarios showed negative shifts in the average minimum
294 pH_{insitu} value (Fig. 7a, c, e).
295 We used Welch's t test to assess the direction of the average minimum and maximum pH_{insitu} trends.
296 For our null hypothesis, we assumed that the population of the trends with an average of −0.0014 yr^{-1}
297 (−0.0024 yr^{-1}) and a standard deviation of 0.0033 yr^{-1} (0.0042 yr^{-1}) was sampled from a population of
298 the minimum (maximum) pH_{insitu} trends with an average trend of 0.0000 yr^{-1} and a standard deviation
299 of 0.0020 yr^{-1}. When the sample size was 289, the *t*-values and the degrees of freedom were 8.7 (6.2)
300 and 412.2 (474.4), respectively. Since the *p* value was less than 0.001, the null hypothesis was rejected.
301 Welch's t test confirmed that the average trends for both the minimum and maximum pH_{insitu} data were
302 negative.
303 We also applied a paired t test to determine whether the two trends calculated from the averaged
304 minimum and maximum pH_{insitu} data were significantly different. The population mean and the sample
305 size were 0.0 and 289, respectively. The *t* value of 4.64 (with 288 degrees of freedom) shows that the
306 null hypothesis was rejected, with the paired t test thus indicating that the two trends calculated from
307 the averaged minimum and maximum pH_{insitu} data were significantly different.
308

4.2 Effects of sampling depth

The WPCL dataset did not discriminate between surface (0.5–2 m) and subsurface (10 m) data when calculating the annual maximum and minimum pH_{insitu}, although monitoring depths were fixed throughout the monitoring period at all the sites. For temperature, the WPCL dataset provided data with the observed depth. Therefore we estimated the percentage possibility that samples were collected at 10 m depth for the quality-controlled datasets with 1481, 1127, and 289 sites, assuming that pH values were measured at the same depth as temperature, and found that samples might have been collected at a depth of 10 m at 13%, 13%, and 15% of the 1481, 1127, and 289 sites, respectively.

Usually the pH is lower in subsurface water than in surface water, as primary production decreases and increases the DIC concentrations in surface and subsurface water, respectively, because of decomposition when Particulate Organic Carbon (POC) is produced by primary producers. We therefore speculate that the annual maximum pH includes very little data from a depth of 10 m, and so this value does represent the winter pH of surface waters. In contrast, the annual minimum pH was somewhat difficult to interpret, as it may have contained data from 10 m at some monitoring sites but only surface data at other sites shallower than 10 m.

Results of statistical analysis (Section 4.1) confirm that the trends in minimum and maximum pH_{insitu} data tended to be negative in the seawater around Japan. The negative tendency of the annual maximum pH_{insitu} trends may imply a trend of overall acidification in winter in surface waters around the Japanese coasts, but the pattern in the annual minimum pH_{insitu} trends was difficult to interpret. Nevertheless,

328 the annual minimum pH_{insitu} trends were, as for the annual maximum pH_{insitu}, also negative (Section
329 3.1) and the trends in the annual minimum pH_{insitu} and in the annual maximum pH_{insitu} showed similar
330 patterns locally (Section 3.2), which indicate that long-term variations in the annual minimum and
331 maximum pH_{insitu} were controlled by the same forcing, so that the pH_{insitu} trends changed in the same
332 direction at both surface and subsurface. Global phenomena such as increases in atmospheric CO_2 and
333 warming of surface water temperatures may cause these forcings.
334
335 ## 4.3 Possible influences on the pH_{insitu} trends in coastal seawater
336 To facilitate our discussion of the factors that influenced the pH_{insitu} trends further, we used the
337 conceptual models of acidification and basification in coastal seawater of Sunda and Cai (2012) and
338 Duarte et al. (2013), as follows:
339 $$PH_{insitu} = \text{Function (D (T), DIC (Air } CO_2\text{, B (T, N)), Alk(S))} \quad (2)$$
340 The pH_{insitu} varies with the ambient temperature (T) on seasonal, inter-annual, and decadal time scales
341 mainly because of changes in the dissociation constants of carbonate and bicarbonate (D(T)) in
342 dissolved inorganic carbon (DIC), alkalinity (Alk), and salinity (S) also affect the pH_{insitu} trends. The
343 solubility pump, which is controlled mainly by atmospheric CO_2 concentration ($AirCO_2$), affects DIC,
344 and ocean acidification occurs when the Air CO_2 increases. Dissolved organic carbon can also be
345 affected by biological processes (B) that depend on the ambient temperature (T) and the nutrient
346 loading (N). There are contrasting relationships between DIC and N in heterotrophic and autotrophic

347 waters. In the waters where organic decomposition is dominated by primary productivity (i.e.
348 autotrophic water), increases in N will enhance primary production and cause DIC to decrease, raising
349 pH (basification). When N increases in the waters adjoining this autotrophic water mass (for example,
350 subsurface waters), POC transport from the autotrophic water mass will also increase, and DIC will
351 increase as POC decomposes (i.e. heterotrophic water), causing acidification (e.g. Sunda and Cai 2012;
352 Duarte et al. 2013). In most coastal region with low terrestrial input, water column productivity is
353 mainly maintained by one-dimensional nutrient cycle: primary production consumes nutrient and DIC
354 to generate POC, and this POC sinks to subsurface and then decomposed in subsurface water and/or
355 seafloor to generate nutrients. As this result, in most coastal stations, surface water becomes
356 autotrophic while subsurface water becomes heterotrophic. In estuary waters and waters near
357 urbanized area with high terrestrial input, however, decomposition of terrestrial POC often overcomes
358 local primary production, and as this result, both surface and subsurface waters become heterotrophic
359 (e.g. Kubo et al. 2017). If we assume that input of terrestrial POC varies in proportion to that of
360 terrestrial N, we can expect that most of these stations show heterotrophic response against N variation.
361 Alkalinity (Alk) generally varies with salinity (S) in coastal oceans and may also affect the pH_{insitu}
362 trend.

363 The DIC process (Air CO_2) of ocean acidification shown in equation 2 generally occurred at all
364 monitoring sites when the Air CO_2 concentrations were horizontally uniform, resulting in overall
365 negative trends in minimum and maximum pH_{insitu}. There was also an overall warming trend in D (T)

366 in Japanese coastal areas, which may have affected the observed pH_{insitu} trend. Both the DIC (Air CO_2)
367 and D (T) may be associated with global processes of warming and ocean acidification, which were
368 triggered by the increases in CO_2 concentrations in the global atmosphere.
369 It is difficult to observe general trends in both DIC (B (T, N)) and Alk (S) at all monitoring sites,
370 because there were no common trends in the factors that control these variables (e.g., salinity of coastal
371 water and terrestrial nutrient loadings) around the Japanese coast in this dataset. The WPCL data
372 contain stations with both autotrophic surface water and heterotrophic subsurface waters, which further
373 obscures the influence of DIC (B (T, N)) on the overall pH_{insitu} trend, as the same trend in B (T, N)
374 leads to opposite trends in DIC (B (T, N) in autotrophic and heterotrophic waters (Duarte et al., 2013).
375 The wide variations in DIC (B (T, N)) and Alk (S) between regions might have caused the regional
376 differences in pH_{insitu} trends among stations, contributing to relatively large standard deviations in both
377 the minimum and maximum pH_{insitu} trends (Fig. 7). The three-step quality control procedures
378 effectively removed the sites with high variability due to analytical errors, and this process may also
379 have removed the effect of large local processes (e.g. heavy phytoplankton bloom, or freshwater
380 discharge change). Nevertheless, we still are able to detect regional scale difference in distribution of
381 positive/negative trends (e.g. Fig.8). Therefore, we discuss the effects of global processes on the
382 overall average pH trends and of regional effects, separately, in later sections (Sections 4.3.1 and 4.3.2).
383

384 ### 4.3.1 Global effects on pH_{insitu} trends

385 Our analysis was based on pH_{insitu} data, so differences observed in trends may reflect long-term
386 changes in water temperature that affected the dissociation constant (process D (T) in equation 2) or
387 changes in the coastal carbon cycle, including absorption of anthropogenic carbon by the solubility
388 pump (process DIC (Air CO_2) in equation 2). Some of the effects of D (T) and DIC (Air CO_2) driven
389 by global warming and ocean acidification may have affected all monitoring sites, and may have
390 contributed to the negative shifts in trend distributions.

391 To evaluate the direct thermal effects related to process D (T) in equation 2, we estimated the pH
392 values normalized to 25°C (pH_{25}), assuming that the minimum (maximum) pH_{insitu} and highest (lowest)
393 temperature and other parameters were measured at the same time. By assuming the other parameters
394 that affected the pH calculation in the CO2sys (Lewis and Wallace 1998, csys.m), such as salinity,
395 DIC, and alkalinity, did not change (these parameters are not measured as part of the WPCL program),
396 we used the method of Lui and Chen (2017) to calculate the pH_{25}, as follows:

397 $$pH_{25} = pH_{insitu} - a_1(T - 25\ °C), \quad (3)$$

398 where a_1 was set to −0.015 and T was the observed temperature.

399 The distributions of the trends in pH_{25} after applying equation 3 are shown in Fig. 10. The minimum
400 and maximum pH_{25} data were normally distributed, meaning that the distributions of the pH_{insitu} trends
401 were maintained after applying equation 3 (Fig. 7e, f). The averages (± standard deviations) of the
402 minimum and maximum pH_{25} trends were −0.0010±0.0032 and −0.0014±0.0041 yr^{-1}, respectively.
403 The averaged trends are consistent with those reported by Midorikawa et al. (2010), who calculated

404 that the pH_{25} decreased at rates of −0.0013 ± 0.0005 yr^{-1} and −0.0018 ± 0.0002 yr^{-1} in summer and
405 winter from 1983 to 2007 along the 137°E line of longitude in the north Pacific. The asymmetry of
406 pH_{25} trends between the minimum and maximum estimates may be related to seasonal variations in
407 pCO_2 and associated asymmetric responses of the air–sea CO_2 flux (Landschutzer et al., 2018;
408 Fassbender et al., 2018).

409 We used Welch's t test to assess the direction of the averages of minimum and maximum pH_{25}
410 trends. The p value was less than 0.001, so the null hypothesis was rejected again. The results of the t
411 test confirm that the average trends for both the minimum and maximum pH_{25} data were also negative,
412 suggesting that the DIC ($AirCO_2$) effect (i.e., ocean acidification) caused the negative shifts in the
413 distribution of the trend for the pH normalized to 25°C.

414 The pH_{25} and pH_{insitu} trends from north to south and from west to east were similar among the
415 prefectures (Fig. 11), except in Miyagi and Tokushima. The trends in the minimum pH_{insitu} and summer
416 pH_{25} were quite similar, but the minimum and maximum pH_{insitu} trends tended to be more negative (by
417 about −0.0010 yr^{-1}) than the corresponding pH_{25} trends, especially in Wakayama, Hiroshioma, Kagawa,
418 and Ehime, which met the threshold number of sampling sites.

419 The average highest temperatures observed at the minimum pH_{insitu} were close to 25 °C in the
420 regions south of Chiba prefecture (Figs. 1 and 12a−d), so the normalization at 25 °C did not have much
421 effect on the minimum pH_{25} in the southern prefectures. In contrast, the maximum pH_{insitu} values were
422 observed at temperatures that were more than 10 °C lower than 25 °C, so the normalization worked

423 well on the winter data. We estimated the temperature trends from the highest and lowest temperatures
424 at the 289 sites that remained after quality control step 3. The trends in the highest and lowest
425 temperatures generally indicated warming, with an average and standard deviation of 0.021±0.040 and
426 0.047±0.036 °C yr^{-1}, respectively (Fig. 13). Estimations from the CO2sys indicate that these warming
427 trends influenced the pH values and were related to the changes of −0.0004 and −0.0010 yr^{-1} in the
428 pH trends in summer and winter, respectively (Fig. 7e−f and 10a−b).
429 We estimated thermal effects and that the pH_{insitu} would change from 8.0150 to 8.0147 in summer
430 and from 8.2568 to 8.2560 in winter, for temperature changes from 25.00 to 25.02 °C, and from 10.00 °
431 to 10.04 °C, respectively, for a salinity of 34, DIC of 1900 millimol m^{-3}, and alkalinity of 2200 millimol
432 m^{-3}. The differences between the pH_{insitu} and the corresponding pH_{25} trends in summer (−0.0004 yr^{-1})
433 and winter (−0.0010 yr^{-1}) can be partly explained by the difference between the decrease in the pH
434 trends in summer (−0.0003 yr^{-1}) and winter (−0.0008 yr^{-1}) arising from the thermal effects.
435
436 ### 4.3.2 Local effects on pH_{insitu} trends
437 We found regional differences in the pH_{insitu} values (e.g. Fig. 6) and pH_{insitu} trends (Figs. 8−9). The
438 negative pH_{insitu} trends (acidification) were more significant in southwestern Japan than in northeastern
439 Japan, especially for the minimum pH_{insitu} data (Fig. 9 and Section 3.2). The JMA (2008, 2018)
440 reported that over the past 100 years, the increase in water temperature in western Japan was ~1.30 °C
441 greater than that in northeastern Japan.

We used CO2sys (Lewis and Wallace 1998) to predict how pH_{insitu} would change under a temperature difference of 0.01 °C yr^{-1} between the northeastern and southwestern areas, and found that pH decreased by 0.0002 (0.0002) yr^{-1} when the temperature changed from 10.00 to 10.01 °C (25.0 to 25.01 °C), assuming a salinity of 34, DIC of 1900 millimol/m^3, and alkalinity of 2200 millimol/m^3. The contrasting trends in the northeast and southwest can be also partly explained by the difference in warming trends (process D (T) in equation 2).

The summer pH_{insitu} is affected by ocean uptake of CO_2 (process DIC in equation 2; Bates et al., 2012; Bates 2014) through long-term changes in biological activity (Cai et al., 2011; Sunda and Cai 2012; Duarte et al., 2013; Yamamoto-Kawai et al., 2015) as well as the effect of changes in the dissociation constant. The responses of pH_{insitu} to changes in marine productivity are, however, complicated.

Previous studies have reported that nutrient loadings in Japan have decreased over recent decades (e.g., Yamamoto-Kawai et al. 2015; Kamohara et al. 2018; Nakai et al. 2018), with variable effects on summer pH_{insitu} in coastal seawater. TN was monitored for a shorter period than pH_{insitu} (1995 to 2009). We assumed that the TN was mainly dissolved inorganic nitrogen and determined the correlations between TN and the minimum and maximum pH_{insitu} trends (Fig. 14). There were statistically significant negative correlations between TN and the minimum (−0.30) and maximum (−0.29) pH_{insitu} trends. Such negative correlation was actually produced by existence of low ΔTN and low ΔpH cluster (eight stations, highlighted by dotted-blue circles in Fig.14). We recognized that the all sites were

461 measured in the same bay, Shimotsu Bay, Wakayama Prefecture. The bay seemed to change volumes
462 of the terrestrial nutrient input during the monitoring period and decreased TN input, resulting in
463 significant basification in the water.

464 For other stations, however, acidification/basification processes seem to occur independently to the
465 changes of TN input. The pH can change even with a constant primary production rate, if a residence
466 time of coastal water changes (for the case of autotropic water, a shorter residence time could cause
467 lower pH). Some parts of stations with significant basification and small ΔTN may have experienced
468 such changes of the water residence time (e.g. artificial changes of the closure rate of inlet, although
469 we have no hydrography data directly proving this assumption at the present time.

470 Nakai et al. (2018) reported that nutrient loadings decreased in the most parts of the Seto Inland Sea
471 from 1981 to 2010, but that several areas remained eutrophic. Because of geographical variations in
472 nutrient loadings and the uneven distribution of autotrophic and heterotrophic stations, there are
473 significant spatial variations in pH trends in the Seto Inland Sea (Fig. 8). The pH trends in coastal areas
474 of western Kyushu, where the anthropogenic nutrient loadings are relatively low, therefore reflect the
475 decreases in nutrient discharges, resulting in variations between regions (e.g., Nakai et al. 2018;
476 Yamamoto and Hanazato 2015; Tsuchiya et al., 2018). Several cities in this area have introduced
477 advanced sewage treatment to prevent eutrophication in coastal seawater (Nakai et al. 2018;
478 Yamamoto and Hanazato 2015).

479 Regional variations in coastal alkalinity along with salinity might be related to changes in land use

and might affect the trends (process Alk(S) in equation 2). Taguchi et al. (2009) measured alkalinity in the surface waters of Ise, Tokyo, and Osaka bays between 2007 and 2009, and reported that total alkalinity was highly correlated with salinity in each bay. For a temperature, salinity, inorganic dissolved carbon, and total alkalinity of 25.00 °C, 35, 1900 millimol m^{-3}, and 2300 millimol m^{-3}, respectively, pH_{insitu} (= pH_{25}) was estimated at 8.1416 using the CO2sys (Lewis and Wallace 1998). By changing the salinity and alkalinity to 34 and 2200 millimol m^{-3}, respectively, pH_{insitu} (= pH_{25}) decreased by 0.0081 to 8.0150. This shows that the pH could deviate significantly from average trends if the inputs of alkaline compounds are changed; consequently, some of our pH trends could have been affected by changing discharge from different land-use types.

Regional differences in pH_{insitu} trends in coastal seawater might be caused by ocean pollution. The speciation and bioavailability of heavy metals change in acidic waters, causing an increase in the biotoxicity of the metals (Zeng et al. 2015; Lacoue-Labarthe et al. 2009; Pascal et al. 2010; Cambell et al. 2014). The rates at which marine organisms photosynthesize and respire in ocean waters decrease and increase, respectively, in water polluted with heavy metals and oils (process DIC in equation 2) because of biotoxicity and eutrophication, thereby resulting in acidification (Hing et al. 2011; Huang et al. 2011; Gilde and Pinckney 2012).

5. Conclusions

499 We estimated the long-term trends in pH_{insitu} in Japanese coastal seawater and examined how the
500 trends varied regionally. The long-term pH_{insitu} data show highly variable trends, although ocean
501 acidification has generally intensified in Japanese coastal seawater. We found that the annual
502 maximum pH_{insitu} at each station, which generally represents the pH of surface waters in winter, had
503 decreased at 75% of the sites and had increased at the remaining 25% of sites. The temporal trend in
504 the annual minimum pH_{insitu}, which generally represents the summer pH in subsurface water at each
505 site, was also similar, but it was relatively difficult to interpret the trends of annual minimum pH_{insitu}
506 because the sampling depths differed between station. The average rate of decrease in the annual
507 maximum pH_{insitu} was -0.0024 yr^{-1}, with relatively large deviations from the average value. Detailed
508 analysis suggests that the decrease in the pH was partly caused by warming of Japanese surface coastal
509 seawater in winter. However, the distributions of the trend in pH normalized to 25°C also showed
510 negative shifts, suggesting that anthropogenic DIC was also increasing in Japanese coastal seawater.
511 There were striking spatial variations in the pH_{insitu} trends. Correlations among the pH_{insitu} time
512 series at different sites revealed that the high variability in the pH_{insitu} trends was not caused by
513 analytical errors in the data but reflected the large spatial variability in the physical and chemical
514 characteristics of coastal environments, such as water temperature, nutrient loadings, and
515 autotropic/heterotrophic conditions. While there was a general tendency towards coastal acidification,
516 there were positive trends in pH_{insitu} at 25%–30% of the monitoring sites, indicating basification, which
517 suggests that the coastal environment might not be completely devastated by acidification. If we can

518 manage the coastal environment effectively (e.g., control nutrient loadings and
519 autotropic/heterotrophic conditions), we might be able to limit, or even reverse, acidification in coastal
520 areas.

521

522 ## Acknowledgments

523 We thank the scientists, captain, officers, and personnel of the National Institute for Environmental
524 Studies, Regional Development Bureau of the Ministry of Land, Infrastructure, Transport and Tourism,
525 who contributed to this study. We acknowledge financial support from the Sasakawa Peace Foundation
526 of the Ocean Policy Research Institute. We also appreciate discussions with members of the
527 Environmental Variability Prediction and Application Research Group of the Japanese Agency for
528 Marine-Earth Science and Technology. Suggestions by two reviewers helped us to improve an earlier
529 version of the manuscript.

530

531 ## References

532 Bates, N. R.: Interannual variability of the ocean CO_2 sink in the subtropical gyre of the North Atlantic
533 Ocean over the last 2 decades, J. Geophys. Res. 112, C09013, doi:10.1029/2006JC003759, 2007.
534 Bates, N. R.: Multi-decadal uptake of carbon dioxide into subtropical mode waters of the North
535 Atlantic Ocean. Biogeosciences 9:2, 649−2, 659, http://dx.doi.org/10.5194/bg-9-2649-2012, 2012.
536 Bates, N. R., Astor, Y. M., Church, M. J., Currie, K., Dore, J. E., Gonzalez-Davila, M., Lorenzoni, L.,
537 Muller-Karger, F., Olafsson, J., and Santana-Casiano, J. M.: A time-series view of changing surface
538 ocean chemistry due to ocean uptake of anthropogenic CO_2 and ocean acidification, Oceanography,

539 27 (1):126−141, http://dx.doi.org/10.5670/oceanog.2014.16, 2014.
540 Bednarsek, N., Tarling, G. A., Bekker, D. C. E., Fielding, S., Jones, E. M., Venables, H. J., Ward, P.,
541 Kuzirian, A., Leze, B., Feely, R. A., and Murphy, E. J.: Extensive dissolution of live pteropods in
542 the Southern Ocean, Nature Geoscience Letter, 5, 881−885, doi: 10.1038/NGEO1635, 2012.
543 Bednarsek, N., Feely, R. A., Reum, J. C. P., Peterson, B., Menkel, J., Alin, S. R., and Hales, B.:
544 *Limacina helicina* shell dissolution as an indicator of declining habitat suitability due to ocean
545 acidification in the California Current Ecosystem, Proc. R. Soc. B, 281 20140123, doi:
546 10.1098/rspb.2014.0123, 2014.
547 Borges, A. V. and Gypen, N.: Carbonate chemistry in the coastal zone responds more strongly to
548 eutrophication than to ocean acidification, Limnology and Oceanography 55: 346−353, 2010.
549 Montagna, R.: Description and quantification of pteropod shell dissolution: a sensitive bioindicator of
550 ocean acidification, Global Change Biology, 18, 2378−2388, doi: 10.1111/j.1365−2486.2012.02668,
551 2012.
552 Byrne, M., Lamare, M., Winter, D., Dworjanyn, S. A., and Uthicke, S.: The stunting effect of a high
553 CO_2 ocean on calcification and development in the urchin larvae, a synthesis from the tropics to the
554 poles, Philosophical Transactions of the Royal Society B, 368, 20120439. Doi:
555 10.1098/rstb.2012.0439, 2013.
556 Cai, W., Hu, X., Huang, W., Murell, M. C., Lehrter, J. C., Lohrenz, S. E., Chou, W., Zhai, W.,
557 Hollibaugh, J. T., Wang, Y., Zhao, P., Guo, X., Gundersen, K., Dai, M., and Gong, G.: Acidification

of subsurface coastal waters enhanced by eutrophication, Nature Geoscience, 4, 766−700, 2011.

Campbell, A. L., Mangan, S., Ellis, R. P., and Lewis, C.: Ocean acidification increases copper toxicity to the early life history stages of the polychaete arenicola marina in artificial seawater, Environ. Sci. Technol. 48, 9745−9753, 2014.

Challener, R. C., Robbins, L. L., and McClintock, J. B.: Variability of the carbonate chemistry in a shallow, seagrass-dominated ecosystem: imprications for ocean acidification experiments, Marine and Freshwater Research, 67, 163−172. Doi:10.1071/MF14219, 2016.

DOE (United States Department of Energy): Handbook of methods for the analysis of the various parameters of the carbon dioxide system in sea water; ver. 2, edited by A. G. Dickson and C. Goyet, ORNL/CDIAC-74, 1994.

Dore, J. E., Lukus, R., Sadler, D. W., Church, M. J. and Karl. D. M.: Physical and biogeochemical modulation of ocean acidification in the central North Pacific, Proc. Natl. Acad. Sci. 106, 12 235−12 240, 2009.

Doney, S.C., Fabry, V. J., Freely, A., and Kleypas, J. A.: Ocean acidification: The other CO_2 program, Annu. Rev. Mar. Sci, 1, 169−192, 2009.

Duarte, C. M., Hendriks, I. E., Moore, T. S., Olsen, Y. S., Steckbauer, A., Ramajo, L., Carstensen, J., Trotter, J. A., and McCullouch, M.: Is ocean acidification an open ocean syndrome? Understanding

575 anthropogenic impacts in seawater pH, Estuaries and Coasts 36, 221−236.doi:10.1007/s12237-013-
576 9594-3, 2013.

577 Fassbender J. A., Rodgers B. K., Palevsky I. H., and Sabine L. C.: Seasonal asymmetry in the evolution
578 of surface ocean pCO_2 and pH thermodynamic drivers and the influence on sea-air CO_2 flux, Global
579 Biogeochemical Cycles, 32, 11476−1497, 2018.

580 Frankignoulle, M., and Bouquegneau, J. M.: Daily and yearly variations of total inorganic carbon in a
581 productive coastal area, Estuarine, Coastal and Shelf Science 30, 79−89, 1990.

582 Gattuso, J. P., and Hansson, L.: Ocean acidification, Oxford Univ. Press, Oxford, 2011.

583 Glide, K., and Pinckney, J. L.: Sublethal effects of crude oil on the community structure of estuarine
584 phytokton, Estuar. Coasts 35, 853−861, 2012.

585 Gonzalez-Davila, M., Santana-Casiano, J. M., and Gonzalez-Davila, E. F.: Interannual variability of
586 the upper ocean carbon cycle in the northeast Atlantic Ocean, Geophys. Res. Lett. 34, L07608,
587 doi:10.1029/2006GL028145, 2007.

588 Hagens, M., Slomp, C. P., Meysman, F. J. R., Seitaj, D., Harlay, J., Borges, A. V., and Middelburg, J.
589 J.: Biogeochemical processes and buffering capacity concurrently affect acidification in a seasonally
590 hypoxic coastal marine basin, Biogeoscience 12, 1561−1583. Doi:10.5194/bg-12-1561-2015, 2015.

591 Hing, L. S., Ford, T., Finch, P., Crane, M., and Morritt, D.: Laboratory stimulation of oil-spill effects
592 on marine phytoplankton, Aquat. Toxicol 103, 32−37, 2011.

593 Huang, Y. J., Jiang, Z. G., Zeng, J. N., Chen, Q. Z., Zhao, Y. Q., Liao, Y. B., Shou, L., and Xu, X. Q.:
594 The chronic effects of oil pollution on marine phytoplankton in a subtropical bay, China. Environ.
595 Monit. Assess. 176, 517−530, 2011.
596 Intergovernmental Panel on Climate Change (IPCC): Climate Change 2013: The Physical Science
597 Basis. Contribution of Working Group I to the Fifth Assessment Report of the Intergovernmental
598 Panel on Climate Change, ed. Stocker, T. F., Qin, D., Plattner, Gian-Kasper., Tignor, M. M. B., Allen,
599 S. K., Boschung, J., Nauels, A., Zia Y., Bex, V., Midgley, P. M., 1−1535 pp. Cambridge,
600 UK: Cambridge University Press, Cambridge, United Kingdom and New York, NY, USA, 2013.
601 Japanese Industrial Standard Z8802 : http://kikakurui.com/z8/Z8802-2011-01.html (in Japanese), 2011.
602 Japanese Meteorological Agency :
603 http://dl.ndl.go.jp/view/download/digidepo_3011050_po_synthesis.pdf?itemId=info%3Andljp%2F
604 pid%2F3011050&contentNo=1&alternativeNo=&__lang=en, 2008.
605 Japanese Meteorological Agency :
606 https://www.data.jma.go.jp/kaiyou/data/shindan/a_1/japan_warm/japan_warm.html (in Japanese),
607 2018.
608 Kamohara, S., Takasu, Y., Yuguchi, M., Mima, N., and Yoshunari, A.: Nutrient decrease in Mikawa
609 Bay, Bulletin of Aichi Fisheries Research Institute 23, 30−32. (in Japanese), 2018.
610 Keeling, C. D., and Whorf, T. P.: Atmospheric CO_2 concentration–Manoa Loa Observatory, Hawaii,
611 1958-1997 (revised August 1998), ORNL NDP−001, Oak Ridge Nathl. Lab. Oak Ridge, TN, 1998.

612 Kubo, A., Maeda, Y., and Kanda, J.: A significant net sink for CO_2 in Tokyo Bay. Nature Scientific
613 Reports 7, 44345, doi:10.1038/srep44355, 2017.
614 Lacou-Labarthe, T., Martin, S., Oberhansli, F., Teyssie, J. L., Jeffree, R., Gattuso, J. P., and
615 Bustamante, P.: Effects of increased pCO_2 and temperature on tracer element (Ag, Cd and Zn)
616 bioaccumulation in the eggs of the common cuttlefish, Sepia officinalis. Biogeosciences 6,
617 2561−2573, 2009.
618 Landschutzer P, Gruber N, Bakker C. E. D., Stemmler I, Six D. K.: Strengthening seasonal marine
619 CO_2 variations due to increasing atmospheric CO_2. Nature Climate Change, 8, 146−150, 2018.
620 Lemasson, A. J., Fletcher, S., Hall-Spence, J. M., and Knights, A. M.: Linking the biological impacts
621 of ocean acidification on oysters to changes in ecosystem services: A review, Journal of Experimental
622 Marine Biology and Ecology, 492, 49−62, 2017.
623 Lewis, E., and Wallace, D. W. R.: Program Developed for CO2 System Calculations. ORNL/CDIAC-
624 105. Carbon Dioxide Information Analysis Center, Oak Ridge National Laboratory, U.S. Department
625 of Energy, Oak Ridge, Tennessee, 1998.
626 Luenberger, D. G.: Optimization by vector space methods, pp. 1-326, John Wiley & Sons, Inc., New
627 York, N.Y, 1969.
628 Lui, H., and Chen, A. C.: Reconciliation of pH_{25} and pH_{insitu} acidification rates of the surface oceans:
629 A simple conversion using only in situ temperature, Limnology and Oceanography: methods, 15,
630 328−355, doi:1002/lom3.10170, 2017.

631 Midorikawa, T., Ishii, M., Sailto, S., Sasano, D., Kosugi, N., Motoi, T., Kamiya, H., Nakadate, A.,
632 Nemoto, K., and Inoue, H.: Decreasing pH trend estimated from 25-yr time series of carbonate
633 parameters in the western North Pacific, Tellus, 62B, 649−659, doi:
634 10.111/j.1600−0889.2010.00474.x, 2010.
635 MIllero, F. (ed): Chemical Oceanography, Fourth Edition. 592pp, CRC Press, New York, United States,
636 2013.
637 Ministry of the Environment: http://www.env.go.jp/hourei/05/000140.html (in Japanese), 2018.
638 Nakai, S., Soga, Y., Sekito, S., Umehara, S., Okuda, T., Ohno, M., Nishijima, W., and Asaoka, S.:
639 Historical changes in primary production in the Seto Inland Sea, Japan, after implementing
640 regulations to control the pollutant loads, Water Policy wp2018093. Doi:10.2166/wp.2018.093, 2018.
641 National Institute for Environmental Studies :
642 https://www.nies.go.jp/igreen/explain/water/content_w.html (in Japanese), 2018.
643 Olafsson, J., Olafsdottir, S. R., Benoit-Cattin, A., Danielsen, M., Arnarson, T. S., and Takahashi, T.:
644 Rate of Iceland Sea acidification from time series measurements, Biogeosciences 6:2, 661−2, 668,
645 http://dx.doi.org/10.5194/bg−6−2661−2009, 2009.
646 Pascal, P. Y., Fleeger, J. W., Galvez, F., and Carman, K. R.: The toxicological interaction between ocean
647 acidity and metals in coastal meiobenthic copepods, Mar. Pollut. Bull, 60, 2201−2208, 2010.
648 Sarmiento, J. L., and Gruber, N.: Ocean Biogeochemical dynamics, pp. 1-503, Princeton Univ. Press,
649 Princeton, New Jersey; Oxfordshire, United Kingdom, 2006.

650 Sunda, W. G., and Cai, W. J.: Eutrophication induced CO_2-acidification of subsurface coastal waters:
651 interactive effects of temperature, salinity, and atmospheric pCO_2, Environ. Sci. Technol. 46,
652 10651−10659, 2012.
653 Taguchi, F., Fujiwara, T., Yamada, Y., Fujita, K., and Sugiyama, M.: Alkalinity in coastal seas around
654 Japan, Bulletin on coastal oceanography, Vol.47, No.1, 71−75, 2009.
655 Yamamoto-Kawai, M., Kawamura, N., Ono, T., Kosugi, N., Kubo, A., Ishii, M., and Kanda, J.: Calcium
656 carbonate saturation and ocean acidification in Tokyo Bay, Japan, J. Oceanogr. 71:427−439, doi
657 10.1007/s10872-015-0302-8, 2015.
658 Tsuchiya, K., Ehara, M., Yasunaga, Y., Nakagawa, Y., Hirahara, M., Kishi, M., Mizubayashi, K.,
659 Kuwahara, V. S., and Toda, T.: Seasonal and Spatial Variation of Nutrients in the Coastal Waters
660 of the Northern G*oto Islands, Japan, Bulletin on coastal oceanography, 55, 125-138. (in*
661 *Japanese),* 2018.
662 Yamamoto, T., and Hanazato, T.: Eutrophication problems of oceans and lakes, -fishes cannot live in
663 clean water, pp. 1−208, ChijinShokan Co. Ltd, ISBN978-4-8052-0885-4, (in Japanese), 2015.
664 Yara, Y., Vogi, M., Fujii, M., Yamano, H., Hauri, C., Steinacher, M., Gruber, N. and Yamano, Y. : Ocean
665 acidification limits temperature-induced poleward expansion of coral habitats around Japan,
666 Biogeosciences, 9, 4955−4968, doi : 10.5194/bg-9-4955-2012, 2012.
667 Zeng, X., Chen, X., and Zhuang, J.: The positive relationship between ocean acidification and pollution,
668 Mar. Poll. Bull, 91, 14−21, 2015.

669 Wakita, M., Nagano, A., Fujiki, T., and Watanabe, S.: Slow acidification of the winter mixed layer in
670 the subarctic western North Pacific, J. Geophys. Res. Oceans, 122, 6923−6935,
671 doi:10.1002/2017JC013002, 2017.
672

673 Figure captions

674

675 Fig. 1 Coastal maps and monitoring sites in Japan. Red points in (a) indicate the fixed sites (n = 1481)
676 monitored by the Regional Development Bureau of the Ministry of Land, Infrastructure, Transport,
677 and Tourism, and the Ministry of the Environment (Japan) under the WCPL monitoring program. (b)
678 Monitoring sites that met the strictest criterion (n = 302).

679

680 Fig. 2 Distributions of the monthly number of data points (N) for (a) maximum and (b) minimum
681 temperatures collected in each prefecture from the 302 most reliable monitoring sites.

682

683 Fig. 3 Examples of (a) acidification (Kahoku Coast in Ishikawa) and (b) basification (Funakoshi Bay
684 in Iwate) trends at monitoring sites. Blue and red colors indicate the annual minimum and maximum
685 pH_{insitu} data and their trends, respectively.

686

687 Fig. 4 Correlations of water temperature and pH_{insitu} at adjacent monitoring sites in the same prefecture.
688 Thin lines denote significant correlations ($\boldsymbol{r}$ = 0.12, degrees of freedom = 283).

689

690 Fig. 5 Scatter plots of correlation coefficients for water temperature and pH_{insitu} at adjacent monitoring
691 sites in the same prefecture. Fig. 5a shows the highest temperature and the minimum pH_{insitu} and Fig.

692 5b shows the lowest temperature and maximum pH_{insitu}, respectively.

693

694 Fig. 6 Examples of time-series for annual minimum and maximum pH_{insitu} data at adjacent monitoring
695 sites close to the boundaries between (a) Osaka and Hyogo and (b) Kagawa and Ehime. Lines of the
696 same color indicate data collected at the same site. Thin and bold lines indicate the annual minimum
697 and maximum pH_{insitu} data, respectively, at each monitoring site. Site locations are included to the
698 right of each panel, with the text color corresponding to the colors in each panel.

699

700 Fig. 7 Histogram of pH trends, represented by ΔpH_{insitu}, showing the slopes of the linear regression
701 lines for the annual minimum (left) and maximum (right) pH_{insitu} data at each monitoring site. The
702 histograms in (a, b), (c, d), and (e, f) show three scenarios: (a, b) all 1481 available sites with
703 continuous records before quality control, (c, d) 1127 sites without outliers, and (e, f) 289 sites that
704 meet the strictest criterion. The trends with statistical significance are denoted by thin color.

705

706 Fig. 8 Distributions of long-term trends in pH_{insitu} (ΔpH_{insitu}/yr) in Japanese coastal seawater. The colors
707 indicate the ranges of acidification (a, c) and basification (b, d). (a, b) and (c, d) are linked to the data
708 used in Figs. 7e and 7f, respectively.

709

710 Fig. 9 (a–b, d–e, g–h, j–k) Average minimum and maximum pH_{insitu} trends (ΔpH_{insitu}/yr) in each

711 prefecture. These figures show each side of the Pacific (a−b), the Seto Inland Sea (d−e), the East
712 China Sea (g−h), and the Japan Sea (j−k). The prefecture names are arranged vertically from eastern
713 (northern) to western (southern) areas. Black shading indicate one standard deviation from the
714 average. (c, f, i, l) Number of monitoring sites in each prefecture and the thin dashed line is the
715 threshold value of 17 (i.e., the average number of monitoring sites in all prefectures). The prefectures
716 that meet the threshold are indicated in purple. The figure is based on the results shown in Figs. 7 (e,
717 f) and 8.
718
719 Fig. 10 Same as Fig. 7, but showing the pH_{25} trends at 289 sites (selected by quality control step 3).
720 The value of pH_{25} was estimated using the method of Lui and Chen (2017).
721
722 Fig. 11 (a−b, d−e, g−h, j−k) Same as Fig. 9, but showing the average estimated minimum and
723 maximum pH_{25} trends (ΔpH_{25}/yr) for each prefecture. Red lines and points indicate the average
724 minimum and maximum pH_{insitu} trends shown in Fig. 9.
725
726 Fig. 12 Average highest and lowest temperatures observed for the minimum and maximum pH_{insitu} data
727 for each prefecture. The blue and red lines and shading indicate the average and one standard
728 deviation from the average, respectively. The prefectures that met the threshold of 17 are shown in
729 purple, as in Figs. 9 (c-l) and 11 (c-l).

730

731 Fig. 13 Same as Fig. 7, but showing the highest and lowest temperature trends at 289 sites (selected
732 by quality control step 3).

733

734 Fig. 14 Correlation between trends in total nitrogen (TN) and trends in (a) minimum and (b) maximum
735 pH_{insitu}. The correlation coefficients are −0.30 and −0.29 for the minimum and maximum pH_{insitu},
736 respectively (significance level of 0.05, r = 0.128; degrees of freedom = 236). Dotted blue circles
737 indicate the data measured in Shimotsu Bay in Wakayama Prefecture.

738

739 Table 1 Number of samples (N) collected at each of the 1481 monitoring sites each year.

740

741 Table 2 Average mutual correlation coefficients among water temperature and pH_{insitu} measurements at
742 adjacent monitoring sites in the same prefecture. The averages were calculated from the data for the
743 highest and lowest temperature, and minimum and maximum pH_{insitu} within 15 km for the three
744 criteria. We refined the sites using three quality control steps, yielding 1481 (step 1), 1127 (step 2),
745 and 302 (step 3) sites. The two columns on the right show the significance level of 5% and the degrees
746 of freedom for the correlation coefficients of each quality check procedure.

747

748

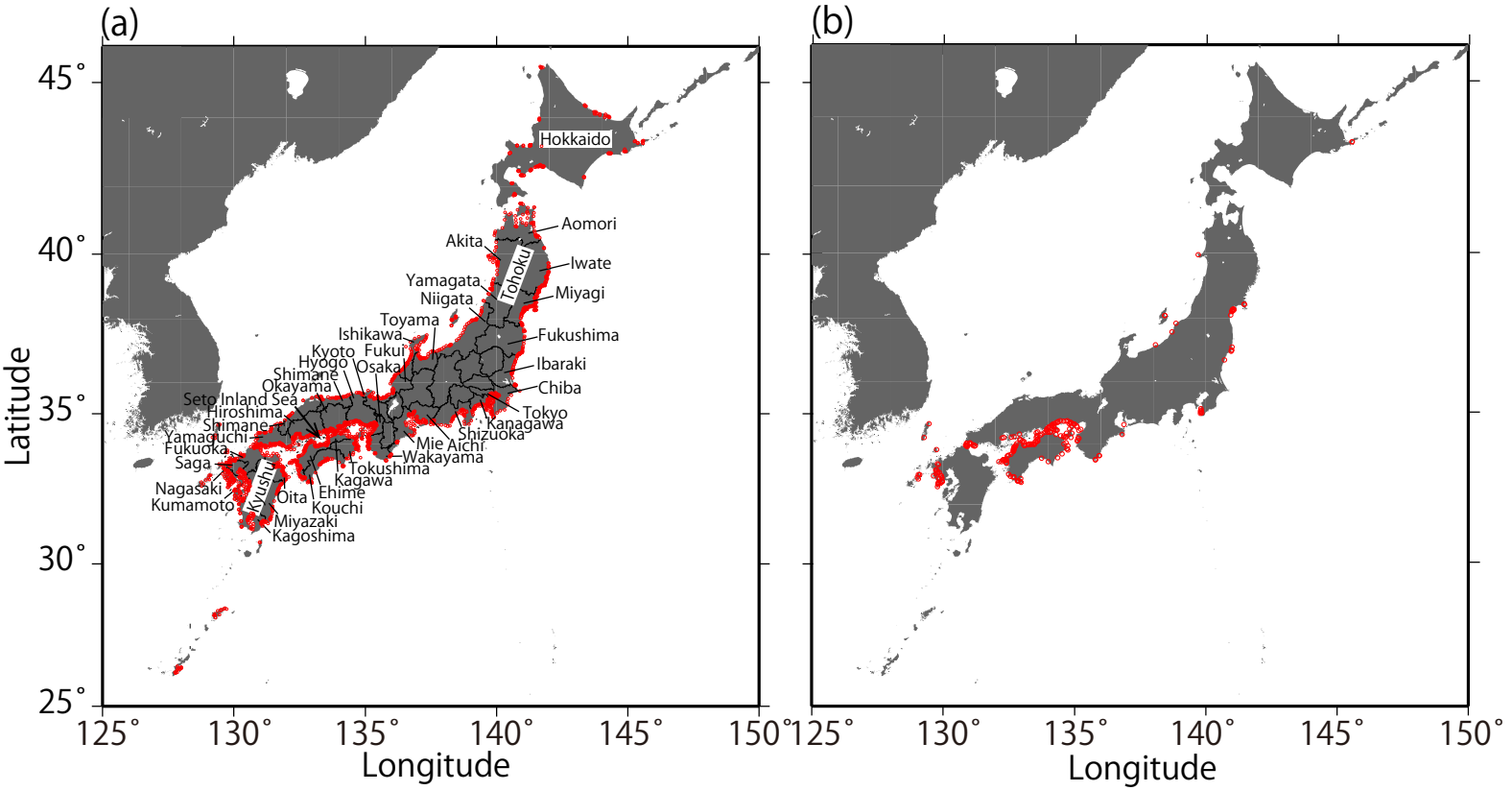

Fig. 1 Coastal maps and monitoring sites in Japan. Red points in (a) indicate the fixed sites (n = 1481) monitored by the Regional Development Bureau of the Ministry of Land, Infrastructure, Transport, and Tourism, and the Ministry of the Environment (Japan) under the WCPL monitoring program. (b) Monitoring sites that met the strictest criterion (n = 302).

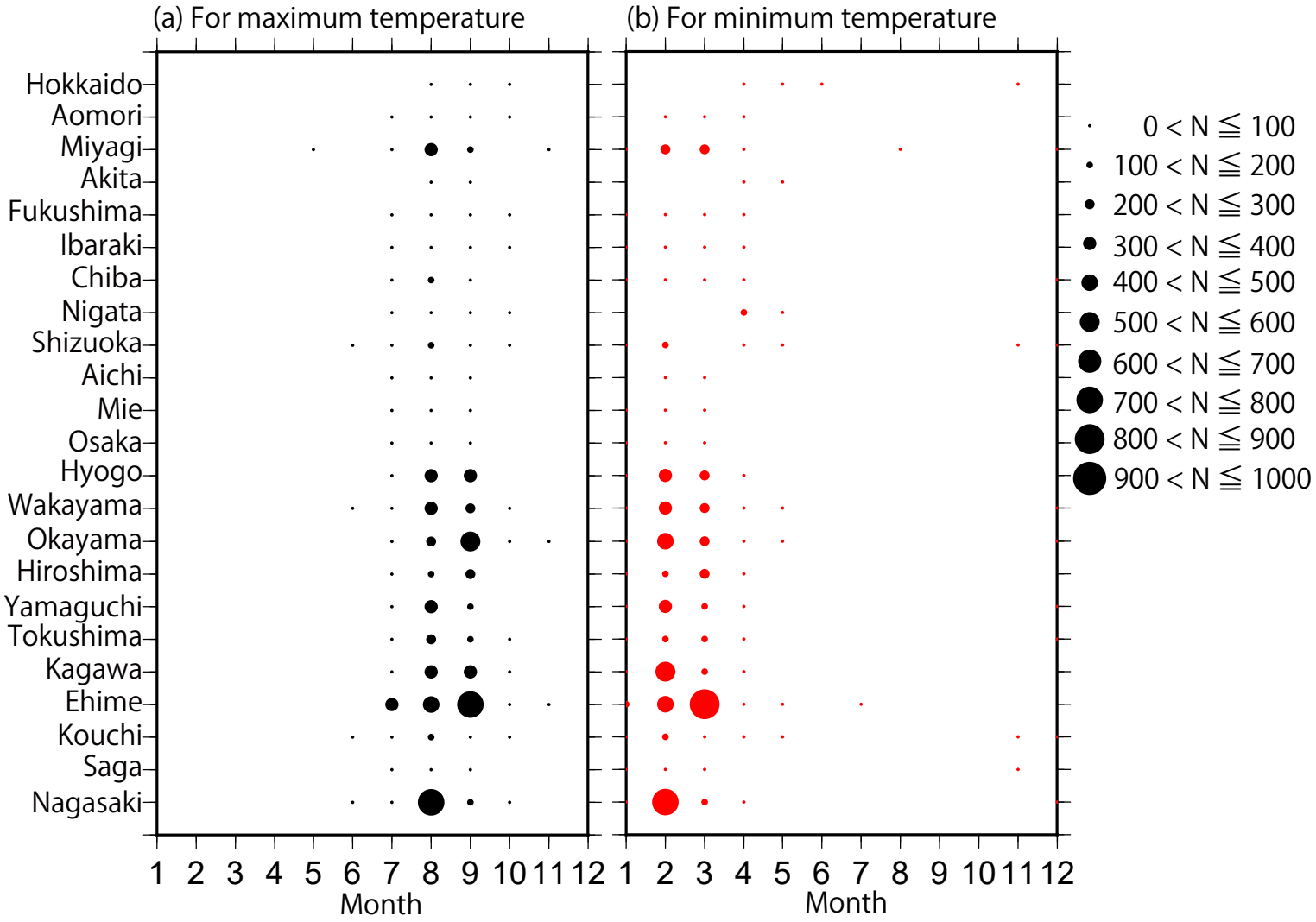

Fig. 2 Distributions of the monthly number of data points (N) for (a) maximum and (b) minimum temperatures collected in each prefecture from the 302 most reliable monitoring sites.

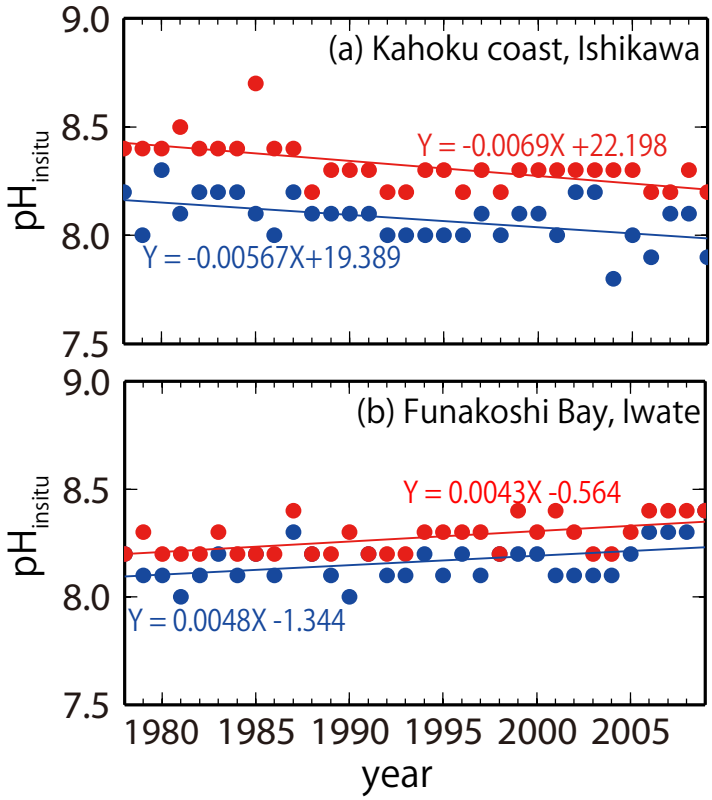

Fig. 3 Examples of (a) acidification (Kahoku Coast in Ishikawa) and (b) basification (Funakoshi Bay in Iwate) trends at monitoring sites. Blue and red colors indicate the annual minimum and maximum pH_{insitu} data and their trends, respectively.

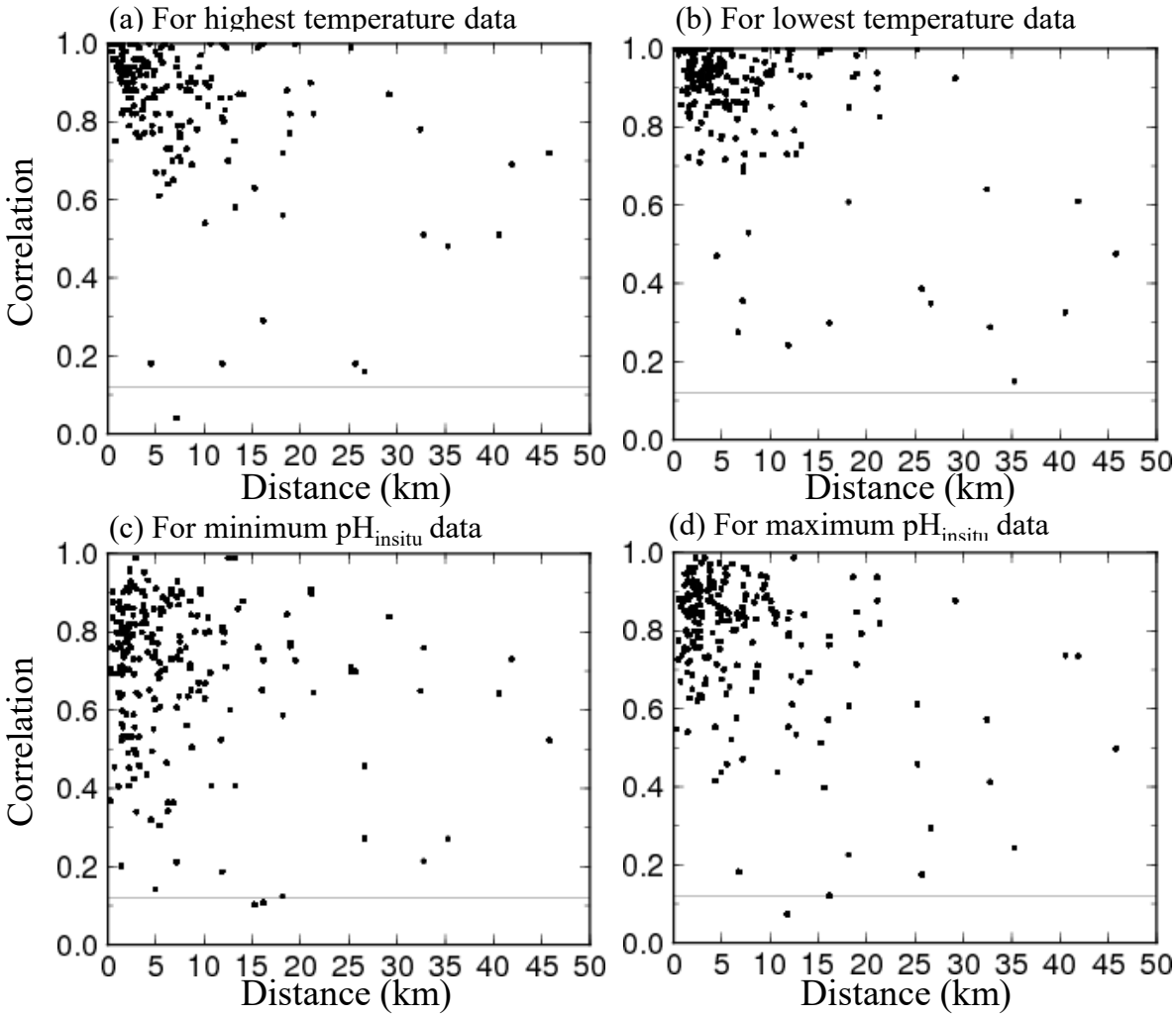

Fig. 4 Correlations of water temperature and pH$_{insitu}$ at adjacent monitoring sites in the same prefecture. Thin lines denote significant correlations ($\boldsymbol{r}$ = 0.12, degrees of freedom = 283).

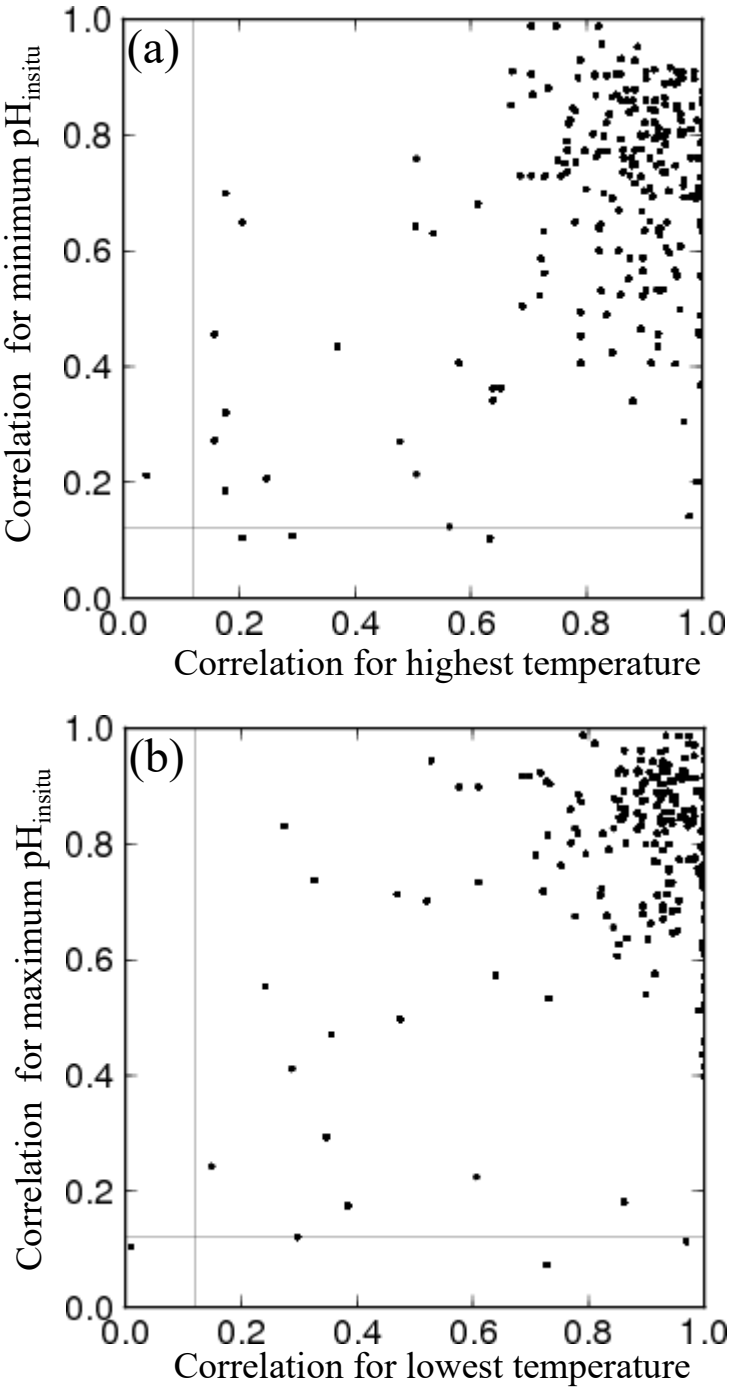

Fig. 5 Scatter plots of correlation coefficients for water temperature and pH_{insitu} at adjacent monitoring sites in the same prefecture. Fig. 5a is for the highest temperature and the minimum $pH_{inisitu}$ data and Fig. 5b for the lowest temperature and the maximum pH_{insitu} data, respectively.

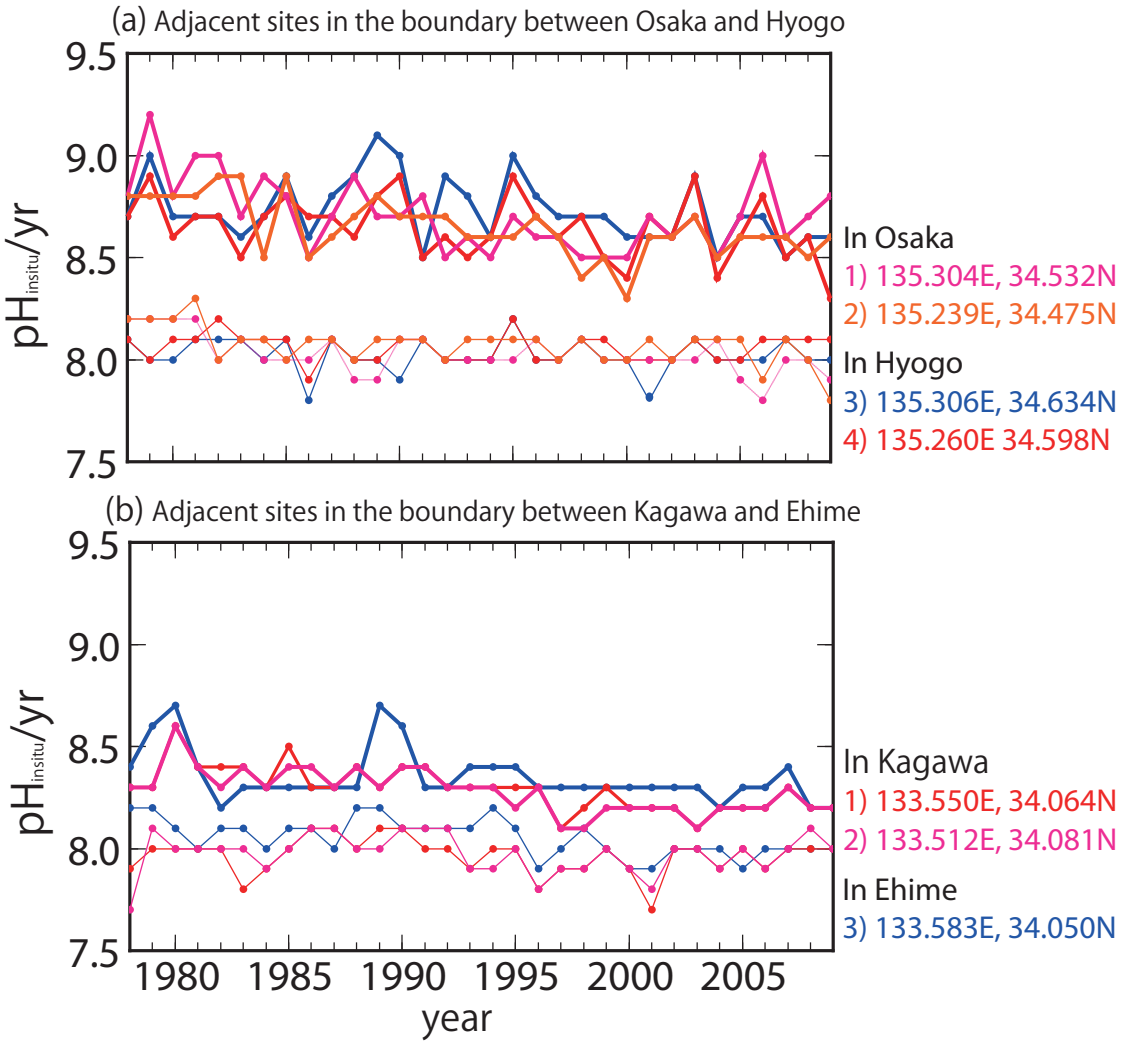

Fig. 6 Examples of time-series for annual minimum and maximum pH_{insitu} data at adjacent monitoring sites close to the boundaries between (a) Osaka and Hyogo and (b) Kagawa and Ehime. Lines of the same color indicate data collected at the same site. Thin and bold lines indicate the annual minimum and maximum pH_{insitu} data, respectively, at each monitoring stations. Site locations are included to the right of each panel, with the text color corresponding to the colors in each panel.

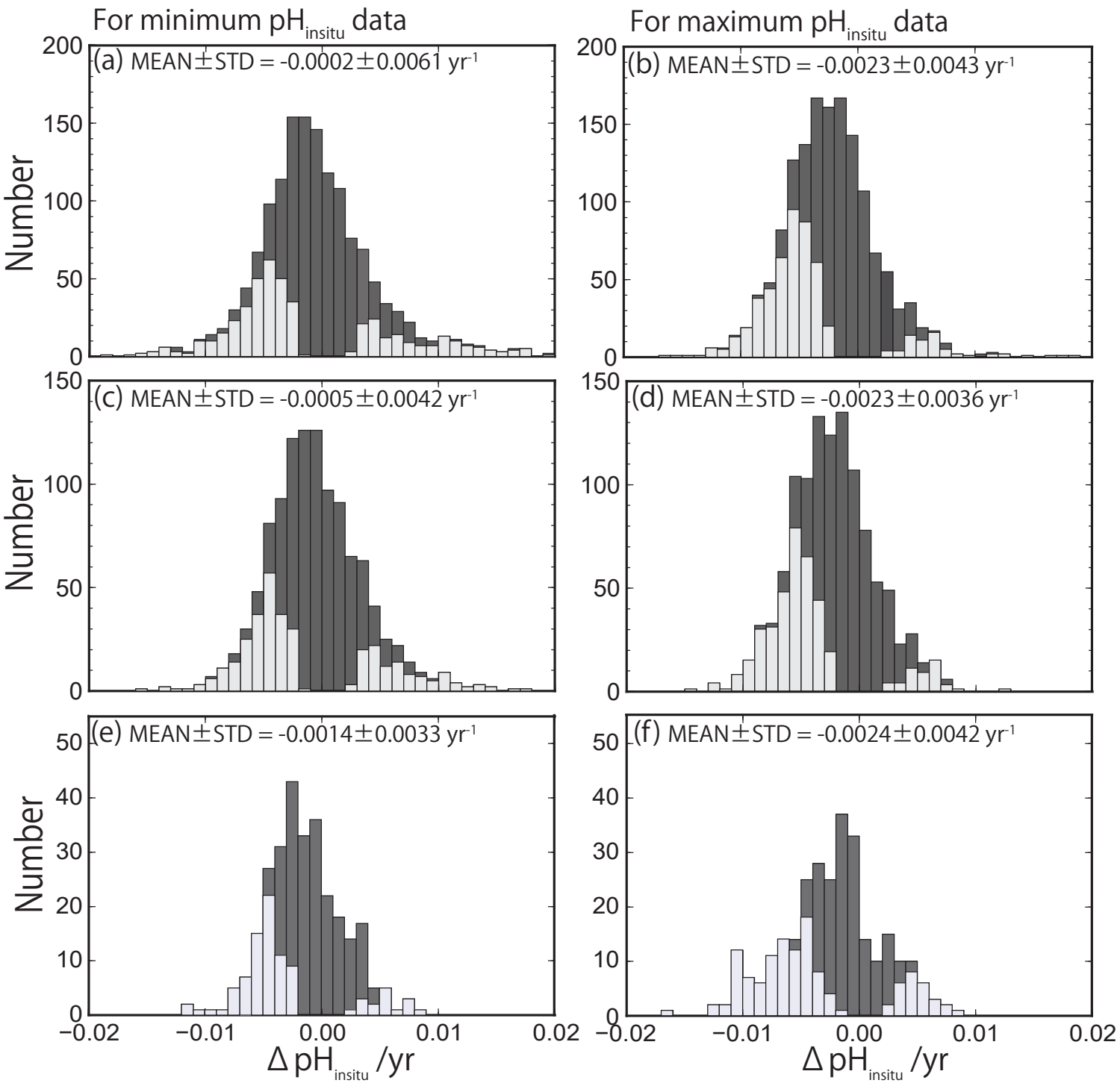

Fig. 7 Histogram of pH trends, represented by ΔpH_{insitu}, showing the slopes of the linear regression lines for the annual minimum (left) and maximum (right) pH_{insitu} data at each monitoring site. The histograms in (a, b), (c, d), and (e, f) show three scenarios: (a, b) all 1481 available sites with continuous records before quality control, (c, d) 1127 sites without outliers, and (e, f) 289 sites that meet the strictest criterion. The trends with statistical significance are denoted by thin color.

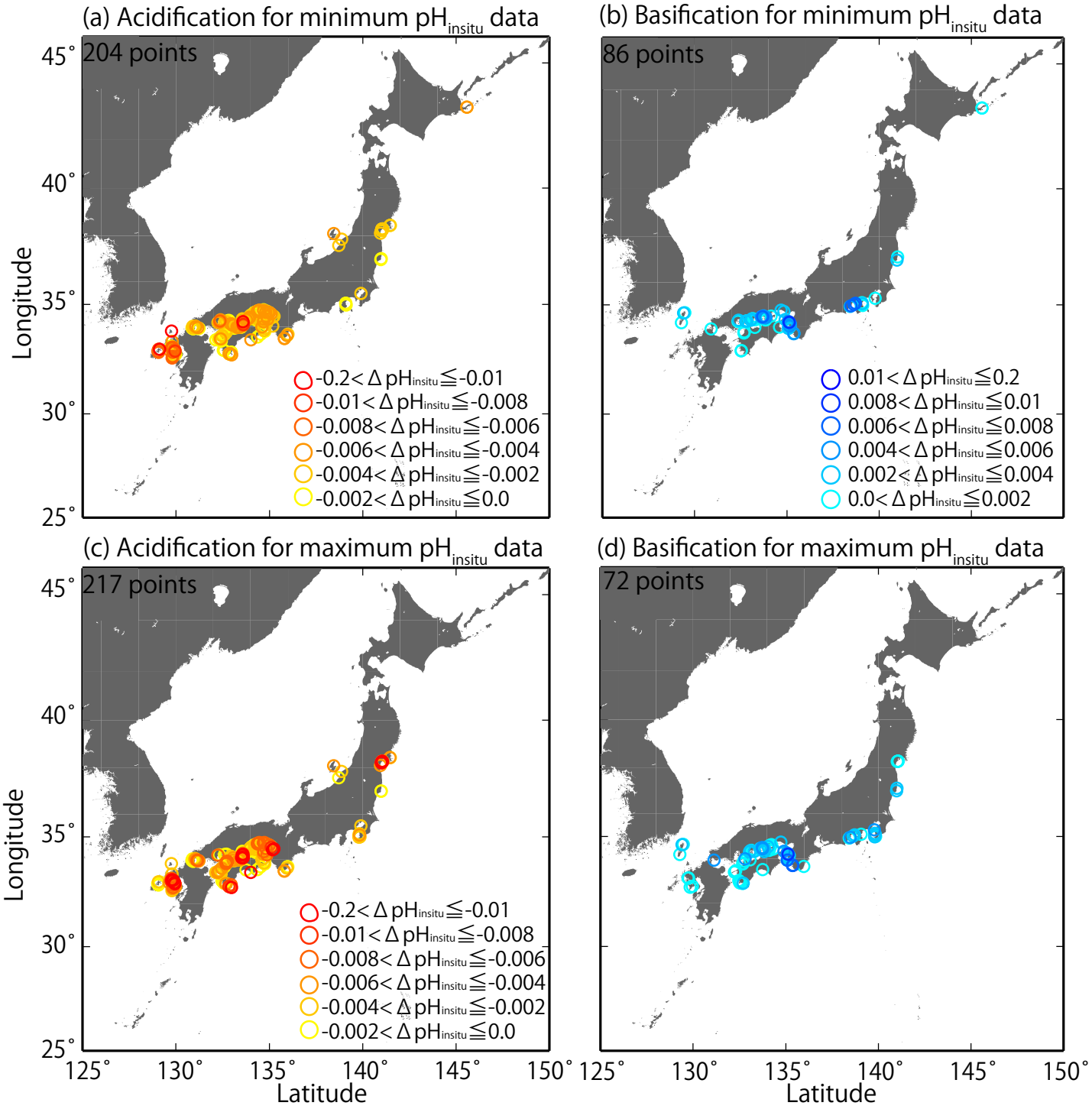

Fig. 8 Distributions of long-term trends in pH$_{insitu}$ (ΔpH$_{insitu}$/yr) in Japanese coastal sea waters. The colors indicate the ranges of acidification (a, c) and basification (b, d). (a, b) and (c, d) are linked to the data used in Figs. 7e and 7f, respectively.

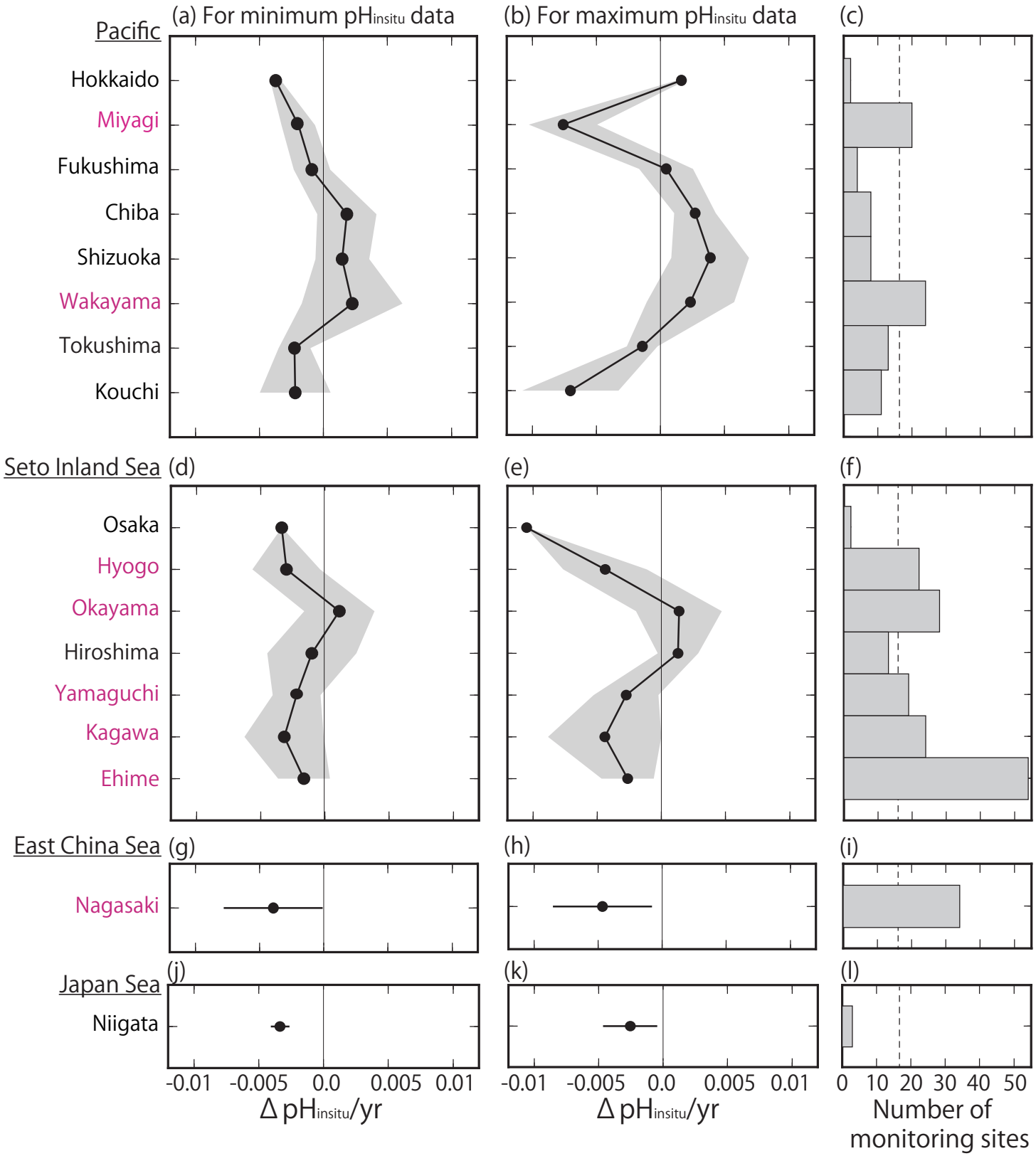

Fig. 9 (a–b, d–e, g–h, j–k) Average minimum and maximum pH_{insitu} trends (ΔpH_{insitu}/yr) in each prefecture. These figures show each side of the Pacific (a–b), the Seto Inland Sea (d–e), the East China Sea (g–h), and the Japan Sea (j–k). The prefecture names are arranged vertically from eastern (northern) to western (southern) areas. Black shading indicate one standard deviation from the average. (c, f, i, l) Number of monitoring sites in each prefecture and the thin dashed line is the threshold value of 17 (i.e., the average number of monitoring sites in all prefectures). The prefectures that meet the threshold are indicated in purple. The figure is based on the results shown in Figs. 7 (e, f) and 8.

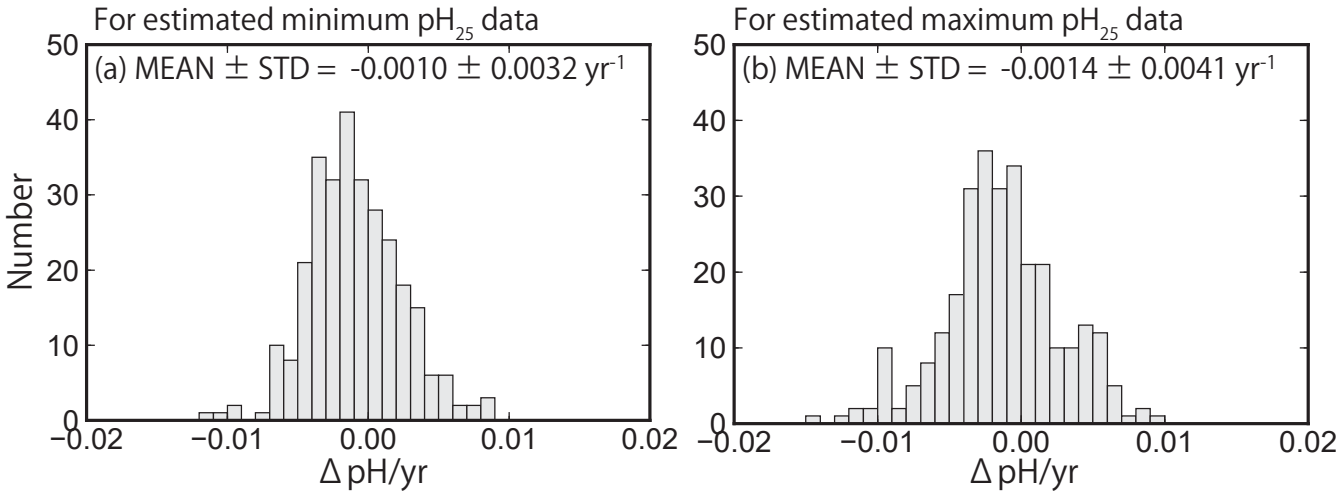

Fig. 10 Same as Fig. 7, but showing the pH_{25} trends at 289 sites (selected by quality control step 3). The value of pH_{25} was estimated using the method of Lui and Chen (2017).

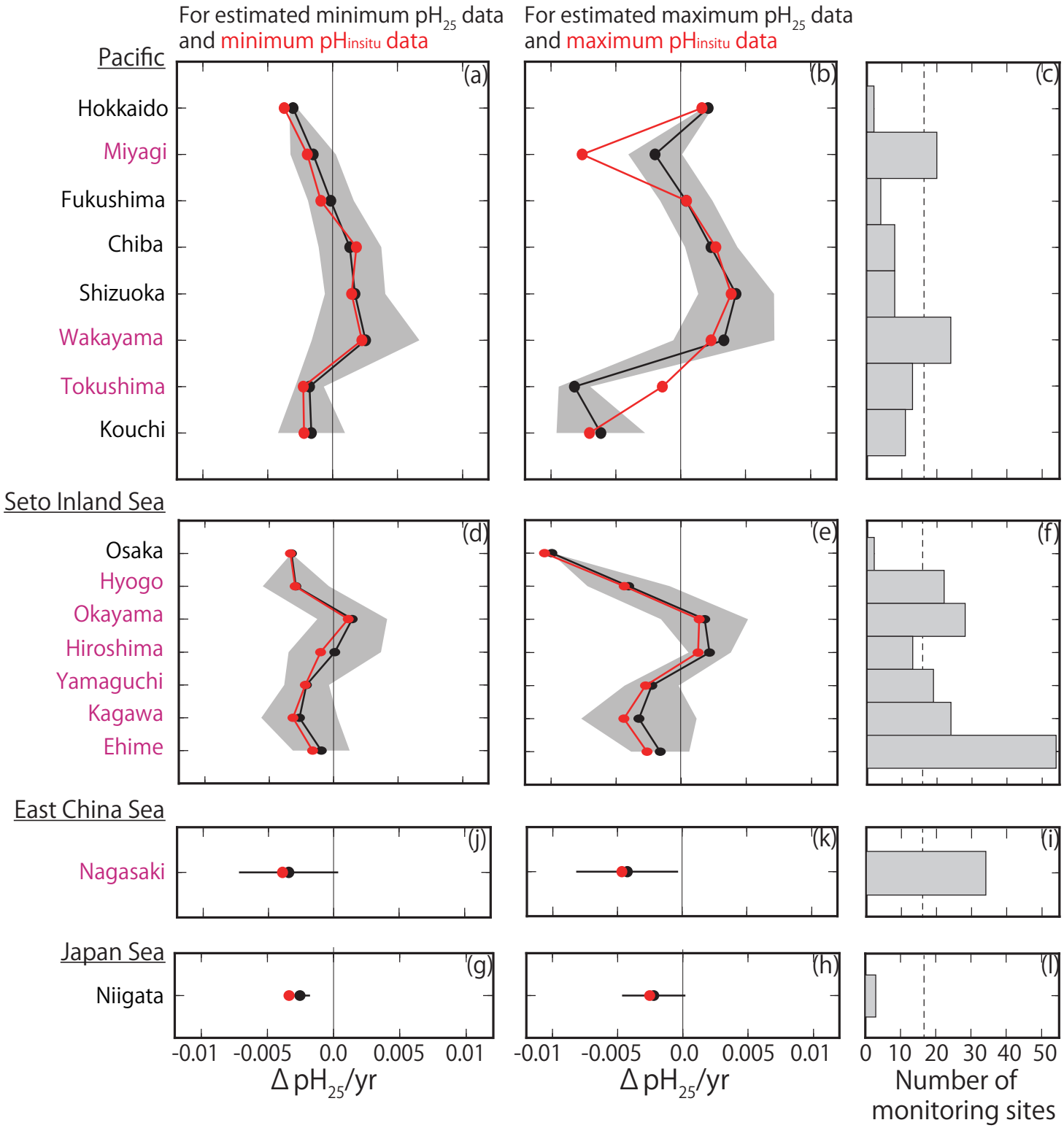

Fig. 11 (a–b, d–e, g–h, j–k) Same as Fig. 9, but showing the average estimated minimum and maximum pH_{25} trends (ΔpH_{25}/yr) for each prefecture. Red lines and points indicate the average minimum and maximum pH_{insitu} trends shown in Fig. 9.

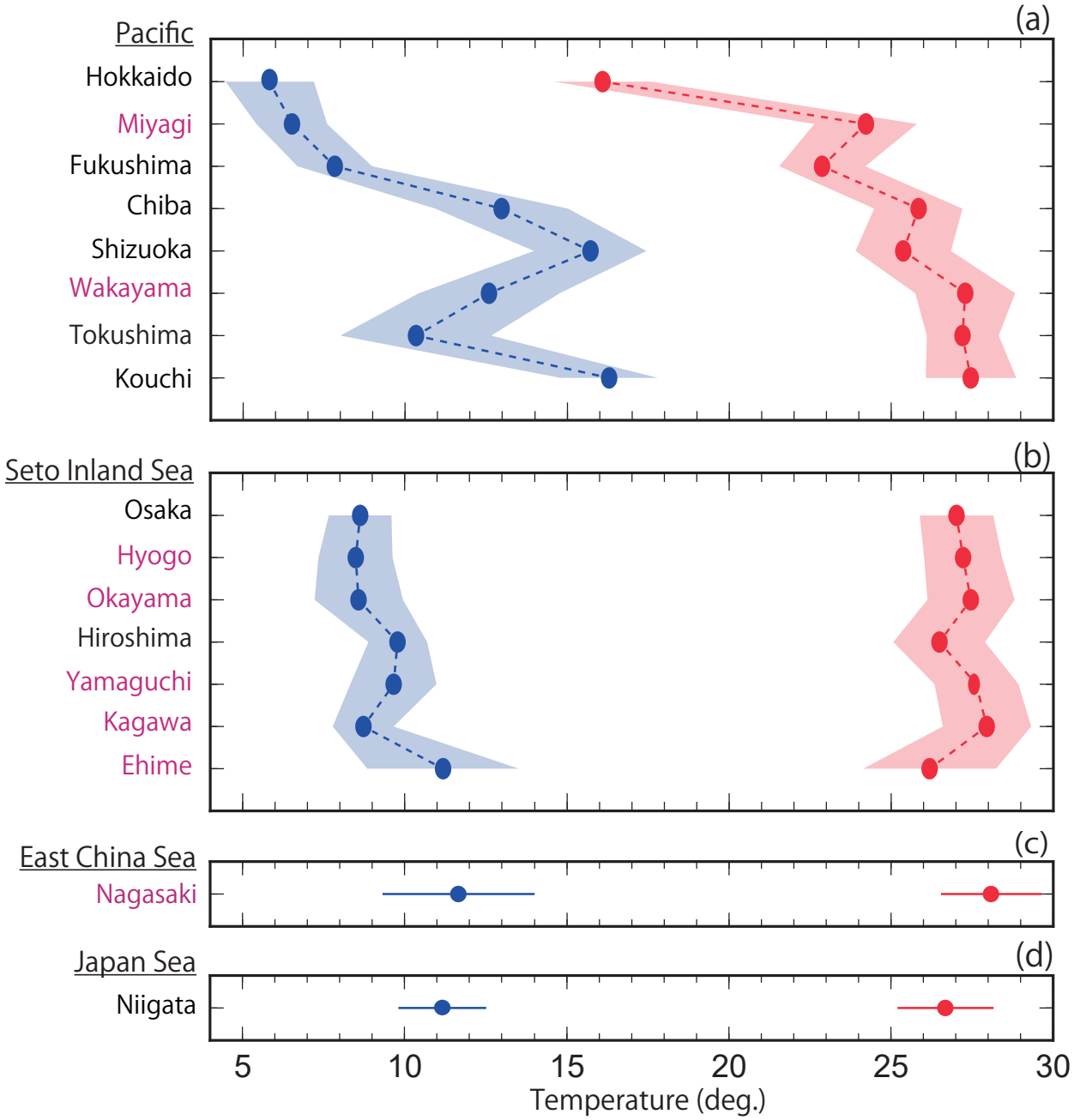

Fig. 12 Average highest and lowest temperatures observed for the minimum and maximum pH_{insitu} data for each prefecture. The blue and red lines and shading indicate the average and one standard deviation from the average, respectively. The prefectures that met the threshold of 17 are shown in purple, as in Figs. 9 (c-l) and 11 (c-l).

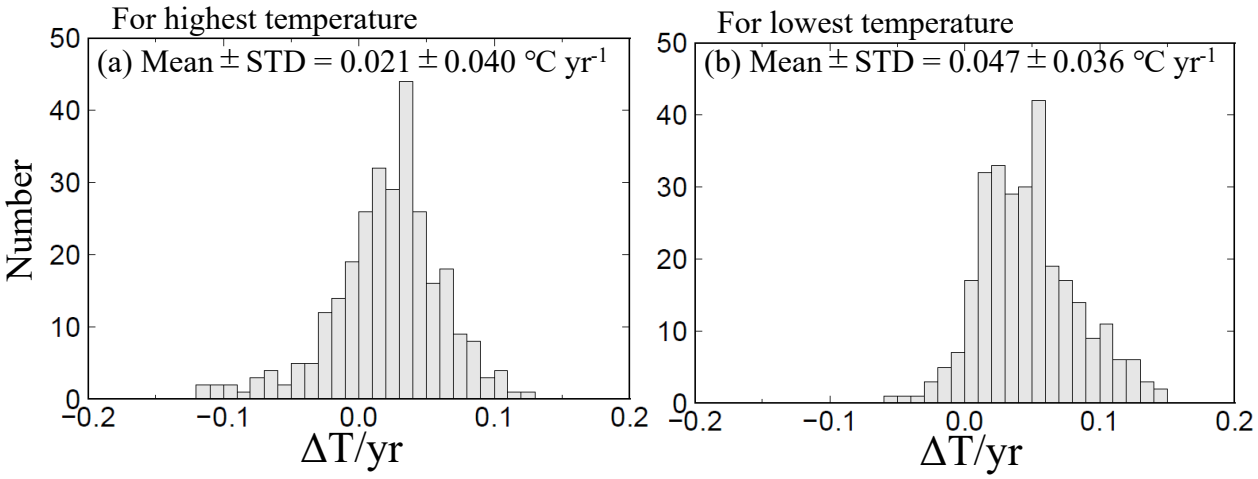

Fig. 13 Same as Fig. 7, but showing the highest and lowest temperature trends at 289 sites (selected by quality control step 3).

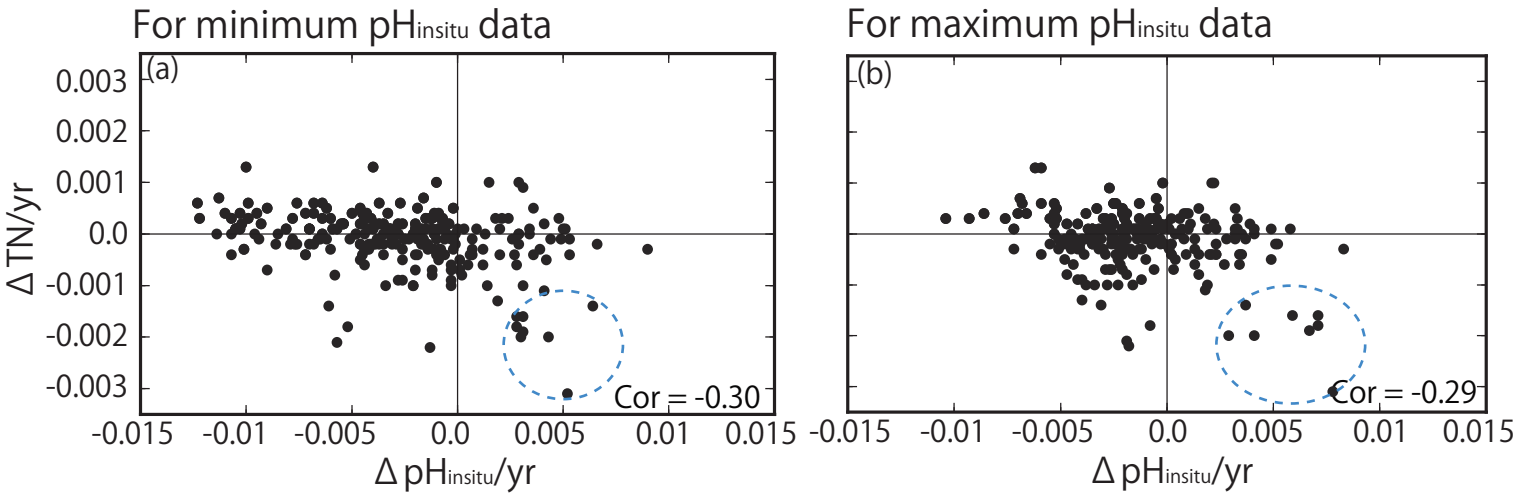

Fig. 14 Correlation between trends in total nitrogen (TN) and trends in (a) minimum and (b) maximum pH_{insitu}. The correlation coefficients are −0.30 and −0.29 for the minimum and maximum pH_{insitu}, respectively (significance level of 0.05, r = 0.128; degrees of freedom = 236). Dotted blue circles indicate the data measured in Shimotsu Bay in Wakayama prefecture.

Table 1 Number of samples (N) collected at each of the 1481 monitoring sites each year.

Year	0≦N＜4	4≦N＜8	8≦N＜12	12≦N＜16	16≦N＜20	20≦N＜24	24≦N＜28	28≦N＜32	32≦N＜40
1978	43	391	83	303	87	15	176	9	4
1979	31	372	73	328	101	19	150	11	7
1980	32	363	88	324	101	15	192	12	5
1981	24	347	72	361	99	13	199	11	3
1982	25	350	74	364	93	9	206	11	4
1983	32	355	75	356	91	11	222	12	0
1984	28	362	74	355	96	10	211	11	3
1985	24	354	86	377	96	9	192	11	8
1986	25	361	81	334	98	8	235	11	9
1987	26	357	78	341	98	4	239	11	1
1988	25	366	74	356	82	6	236	11	2
1989	26	365	83	344	84	5	238	17	3
1990	24	377	76	347	83	1	238	14	5
1991	24	367	80	355	93	5	226	13	5
1992	24	367	79	352	95	1	230	16	0
1993	17	374	76	357	94	8	225	14	0
1994	17	376	85	347	102	24	208	14	3
1995	29	376	109	311	104	3	227	12	0
1996	19	419	80	307	104	4	226	14	1
1997	20	396	82	315	115	5	225	13	0
1998	16	389	103	325	99	0	225	12	0
1999	17	396	68	381	67	2	224	12	7
2000	17	389	82	376	72	1	231	6	2
2001	17	392	90	382	50	8	220	6	1
2002	17	368	102	392	49	1	229	7	0
2003	17	365	93	402	51	1	233	6	1
2004	17	370	84	400	50	1	240	5	2
2005	16	354	152	356	46	9	228	3	0
2006	16	370	134	345	50	0	244	5	3
2007	17	399	128	353	62	0	202	5	3
2008	17	402	128	350	64	0	211	5	1
2009	17	403	143	340	58	0	217	5	8

Table 2 Average mutual correlation coefficients among water temperature and pH_{insitu} measurements at adjacent monitoring sites in the same prefecture. The averages were calculated from the data for the highest and lowest temperature, and minimum and maximum pH_{insitu} within 15 km for the three criteria. We refined the sites using three quality control steps, yielding 1481 (step 1), 1127 (step 2), and 302 (step 3) sites. Two right columns represent a significant level of 5% and a degree of freedom for the correlation coefficients of each quality check procedure.

Quality check procedue	highest temperature data	lowest temperature data	minimum pH_{insitu} data	maximum pH_{insitu} data	Significance level of 5%	Degree of freedom
1	0.79	0.78	0.51	0.64	0.10	386
2	0.80	0.79	0.54	0.69	0.15	170
3	0.85	0.87	0.62	0.72	0.25	59